Marine Pollution Bulletin 217 (2025) 118140

Contents lists available at ScienceDirect

Marine Pollution Bulletin

journal homepage: www.elsevier.com/locate/marpolbul

Distributions and compositional characteristics of per- and polyfluoroalkyl substances (PFASs) in sediments of the regional seas of South Korea☆

Sunmi Yang [a], Jiyun Gwak [a], Jihyun Cha [a], Kiho Park [a], Youngnam Kim [a], Sea-Yong Kim [b], Yeonjung Lee [c], Dong Han Choi [c], Kongtae Ra [d], Hyo-Bang Moon [e], Seongjin Hong [a,*]

[a] Department of Earth, Environmental & Space Sciences, Chungnam National University, Daejeon 34134, Republic of Korea
[b] Department of Biology, Chungbuk National University, Cheongju 28644, Republic of Korea
[c] Ocean Climate Response & Ecosystem Research Department, Korea Institute of Ocean Science and Technology, Busan 49111, Republic of Korea
[d] Marine Environment Research Department, Korea Institute of Ocean Science and Technology, Busan 49111, Republic of Korea
[e] Department of Marine Science and Convergence Engineering, College of Science and Convergence Technology, Hanyang University, Ansan 15588, Republic of Korea

ARTICLE INFO

Keywords:
PFASs
Sediment
Vertical profile
Ocean dumping
Partition coefficient
HPLC-MS/MS

ABSTRACT

This study investigated the distribution and composition of 28 per- and polyfluoroalkyl substances (PFASs) in surface and core sediments from the regional seas of South Korea. Surface sediments were collected from the Yellow Sea (YS, n = 10), East China Sea (ECS, n = 6), South Sea (SS, n = 5), and East Sea (ES, n = 12), and core sediments were obtained from the ES (n = 3, 0–30 cm). Sediment samples were extracted with methanol by shaking, followed by purification using solid-phase extraction cartridges. The purified extracts were then analyzed using high-performance liquid chromatography–tandem mass spectrometry (HPLC–MS/MS) to quantify 11 perfluoroalkyl carboxylic acids, 9 perfluoroalkyl sulfonic acids, 5 precursors, and 3 emerging PFASs. The highest PFAS concentrations in surface sediments were observed in the YS (300 ng g^{-1} organic carbon (OC)), followed by the ES (150 ng g^{-1} OC), ECS (120 ng g^{-1} OC), and SS (14 ng g^{-1} OC). Core sediment analysis revealed the accumulation of PFASs within the top 10 cm depth at the dumpsite, along with elevated OC contents (2.7–4.4 %) and lighter carbon stable isotope ratios ($\delta^{13}C$, −23 to −22 ‰) indicating the influence of dumped wastes. Principal component analysis classified the sites into three groups based on chemical composition, reflecting regional differences in PFASs usage, transport, and deposition. These findings provide critical insights into the distribution and environmental behavior of PFASs in marine sediments and contribute to developing future regulatory frameworks and pollution management strategies.

1. Introduction

Per- and polyfluoroalkyl substances (PFASs) are synthetic chemicals widely used in industrial and consumer products due to their water- and oil-repellent properties (D'Eon and Mabury, 2011). They are synthesized primarily via electrochemical fluorination and telomerization processes and are structurally characterized by strong carbon-fluorine bonds, which confer high thermal and chemical stability (D'Eon and Mabury, 2011; Jiang et al., 2024). Due to increasing concerns over their environmental persistence and potential health risks, long-chain PFASs such as perfluorooctanoic acid (PFOA), and perfluorooctane sulfonic acid (PFOS) have been regulated under the Stockholm Convention (UNEP, 2010, 2019). However, emerging alternatives, including short-chain PFASs and precursors, have also demonstrated notable persistence and toxicity in environmental systems (Wang et al., 2015; Munoz et al., 2019).

PFASs are directly discharged from various industrial and domestic sources into river systems and are readily transported through aqueous pathways. Although these are distributed across multiple environmental media, they ultimately undergo transport to the open sea, where they accumulate and are sequestered in marine sediments (Li et al., 2018b; Wang et al., 2022; Zheng et al., 2017). Marine sediments, recognized as important reservoirs of PFASs, reflect their presence in seawater through interactions with ocean currents and the water column. Additionally, sediments provide a hydrophobic medium that facilitates the accumulation of organic pollutants (Gao et al., 2014). The contamination of

☆ This article is part of a Special issue entitled: 'YES2023' published in Marine Pollution Bulletin.

* Corresponding author.
E-mail address: hongseongjin@cnu.ac.kr (S. Hong).

https://doi.org/10.1016/j.marpolbul.2025.118140
Received 14 March 2025; Received in revised form 29 April 2025; Accepted 9 May 2025
Available online 14 May 2025

sediments with PFASs poses potential risks not only to aquatic organisms but also to the broader marine ecosystem and human health (Diao et al., 2022; Gao et al., 2014; Hu et al., 2025; Kennicutt, 2017). Thus, understanding the distribution and behavior of PFAS precursors and substitutes in sediments is very important, but related studies are lacking.

In South Korea, most studies on PFASs distribution have focused on freshwater systems, estuaries, and semi-enclosed bays, while little is known about their occurrence and behavior in regional seas (Lee et al., 2020a; Mussabek et al., 2020; Shen et al., 2018). Regional seas serve as transitional zones connecting estuaries, coastal areas, and the open ocean. Understanding the distribution, behavior, and accumulation of pollutants in regional seas is essential for elucidating the long-distance transport of land-derived contaminants. Notably, South Korea allowed the ocean dumping of land-based waste between 1988 and 2016 at three designated marine dumpsites located in the Yellow Sea (YS) and East Sea (ES) (Eo et al., 2022; MOF, 2015; Chung et al., 2020). These areas have been found to contain high levels of anthropogenic pollutants, yet to date, no PFASs-specific assessments have been conducted (Hong and Shin, 2009; Jung et al., 2023).

This study investigated the distribution and compositional characteristics of 28 PFASs, including legacy compounds, emerging alternatives, and known precursors, in surface sediments from the regional seas surrounding the Korean Peninsula [YS, East China Sea (ECS), South Sea (SS), and ES]. Additionally, the contamination history of PFASs was examined through core sediment analysis in the ES, including designated waste dumpsites. Principal component analysis (PCA) was conducted to assess the composition of PFASs, providing insights into their behavior, fate, and potential sources. The levels of PFAS contamination in sediments from the regional seas of Korea are expected to reflect inputs from riverine and estuarine inflows, as well as the impacts of historical ocean dumping. The results provide critical baseline data for understanding PFAS contamination trends in Korean regional seas and support the development of future environmental monitoring and management strategies.

2. Materials and methods

2.1. Study area, sampling, and sample preparation

A total of 33 surface sediment samples were collected from the YS (Y1–Y10, n = 10), ECS (EC1–EC6, n = 6), SS (S1–S5, n = 5), and ES (C1–C12, n = 12) during three separate sampling campaigns conducted in January 2024, May 2023, and April 2023, respectively, using the research vessels ISABU, NARA, and Onnuri (Fig. 1). In addition, core sediment samples were collected from three sites in the ES (C1, C3, and C6), located near two designated ocean dumping sites, "Byeong." The sampling sites in this study were selected to provide an overall assessment of PFASs contamination in regional marine sediments, due to the limited availability of prior data on their distribution and levels. However, waste dumpsites were specifically included as targeted survey sites, as they were considered potential hotspots for anthropogenic pollutants. Each regional sea varies in geographic area and water depth. Thus, the number and locations of sampling sites were determined based on the characteristics of each region. At least five sampling sites were selected to adequately represent each regional sea. A detailed list of collected samples is provided in Table S1 of the Supplementary Materials. Surface sediments (0–1 cm) and core sediments (0–30 cm) were collected using grab samplers and box core samplers, respectively. All materials that could potentially come into contact with the sample during collection and extraction were made of polypropylene (PP). The use of polytetrafluoroethylene (PTFE) and glass materials was avoided to minimize background contamination by PFASs. All sediment samples were stored at −20 °C until analysis.

2.2. Organic carbon, total nitrogen, and stable isotopes analysis

To measure organic carbon (OC) and total nitrogen (TN) in sediment samples, 1 g of freeze-dried and homogenized sediment was placed in a 15 mL PP tube, followed by the addition of 1 M hydrochloric acid to remove inorganic carbon (Kim et al., 2018). Stable isotope analysis of OC and TN was conducted using an elemental analyzer (EA; Vario ISOTOPE cube, Elementar, Hanau, Germany) coupled with isotope ratio mass spectrometry (IRMS; Isoprime VisION, Elementar, Manchester, UK).

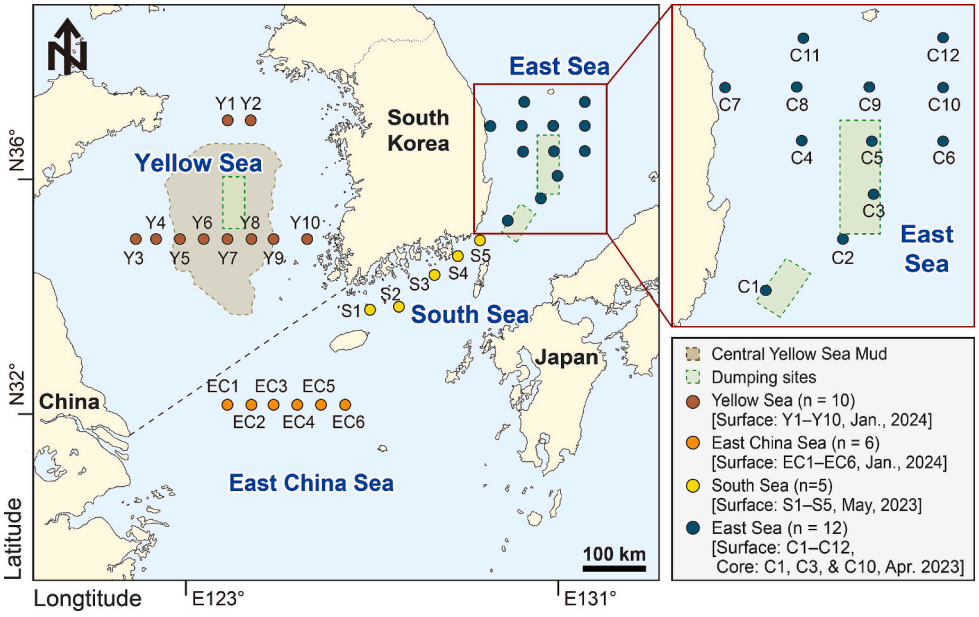

Fig. 1. Map showing the sampling sites for surface and core sediments in the regional seas surrounding South Korea, including the Yellow Sea (Y1–Y10), East China Sea (EC1–EC6), South Sea (S1–S5), and East Sea (C1–C12). Surface sediments were collected from all sites, and core sediments were collected from sites C1, C3, and C10 in the East Sea.

2.3. PFASs analysis

Standard materials of 28 PFASs were used in this study, comprising 11 perfluoroalkyl carboxylic acids (PFCAs, C_4–C_{14}), 9 perfluoroalkyl sulfonic acids (PFSAs, C_4–C_{10}), 5 precursors, and 3 emerging PFASs. The PFCAs included perfluorobutanoic acid (PFBA), perfluoropentanoic acid (PFPeA), perfluorohexanoic acid (PFHxA), perfluoroheptanoic acid (PFHpA), PFOA, perfluorononanoic acid (PFNA), perfluorodecanoic acid (PFDA), perfluoroundecanoic acid (PFUnDA), perfluorododecanoic acid (PFDoDA), perfluorotridecanoic acid (PFTriDA), and perfluorotetradecanoic acid (PFTeDA). The PFSAs included linear perfluorobutane sulfonate (L-PFBS), L-perfluoropentane sulfonate (L-PFPeS), L-perfluorohexane sulfonate (L-PFHxS), branched PFHxS (br-PFHxS), L-perfluoroheptane sulfonate (L-PFHpS), L-PFOS, br-PFOS, L-perfluorononane sulfonate (L-PFNS), and L-perfluorodecane sulfonate (L-PFDS). The precursors included *N*-methylperfluoro-1-octanesulfonamidoacetic acid (N-MeFOSAA), N-ethylperfluoro-1-octanesulfonamidoacetic acid (N-EtFOSAA), 1H,1H,2H,2H-perfluorohexanesulfonate (4:2 FTS), 1H,1H,2H,2H-perfluorooctanesulfonate (6:2 FTS), and 1H,1H,2H,2H-perfluorodecanesulfonate (8:2 FTS). Emerging PFASs were included 2,3,3,3-tetrafluoro-2-(1,1,2,2,3,3,3-heptafluoropropoxy)-propanoic acid (GenX), dodecafluoro-3H-4,8-dioxanonanoate (ADONA), and 9-chlorohexadecafluoro-3-oxanonane sulfonate (F53B) (Table 1). Most PFASs were included in the PFAC-MXH standard mixture, while GenX, NaDONA, F53B, L-PFHxS, and L-PFOS were purchased individually. Mass-labeled standard mixtures (MPFAC-MXA) were used as internal standards (IS). All standards (purity >98 %) were obtained from Wellington Laboratories (Guelph, Ontario, Canada). Full details of all target compounds, including their names and abbreviations, are provided in Table S2. These standards were selected to cover a broad range of PFAS structures, encompassing both short-chain alternatives and legacy long-chain compounds, thus enabling comprehensive monitoring of environmentally relevant PFASs.

The extraction and purification of sediment samples were conducted with modifications to the previously established method (Lee et al., 2020a) (Fig. S1). A 5 g of freeze-dried and sieved (2-mm mesh) sediment was transferred to a 50 mL PP tube, and 5 ng of ISs were added. Next, 10 mL of methanol was added, and the sample was subjected to mechanical shaking at 250 rpm for 30 min, followed by sonication for 30 min to facilitate organic extraction. The mixture was then centrifuged at 3000 rpm for 20 min to separate the supernatant. The sediment was extracted twice more using the same procedure. The supernatants were combined and concentrated to 1 mL under a gentle N_2 gas flow. Purification was carried out using ENVI-Carb cartridges (100 mg, 1 cc, Sigma-Aldrich, St.

Table 1
Concentration ranges and detection rates of 28 PFASs in surface sediments from the regional seas of South Korea.

Compounds	LOQ (ng g^{-1} dw)	Yellow Sea			East China Sea			South Sea			East Sea		
		DR (%)[a]	Min to Max (ng g^{-1} OC)	Mean (ng g^{-1} OC)	DR (%)	Min to Max (ng g^{-1} OC)	Mean (ng g^{-1} OC)	DR (%)	Min to Max (ng g^{-1} OC)	Mean (ng g^{-1} OC)	DR (%)	Min to Max (ng g^{-1} OC)	Mean (ng g^{-1} OC)
PFCAs													
PFBA	0.22	0	–	–	0	–	–	0	–[c]	–	0	–	–
PFPeA	0.10	0	–	–	0	–	–	0	–	–	0	–	–
PFHxA	0.04	10	<LOQ[b] to 11	1.1	0	–	–	0	–	–	67	<LOQ to 3.5	1.4
PFHpA	0.02	80	<LOQ to 11	4.0	0	–	–	0	–	–	83	<LOQ to 7.5	3.6
PFOA	0.06	100	46 to 610	200	100	41 to 110	73	60	<LOQ to 12	6.8	100	7.0 to 62	18
PFNA	0.08	90	<LOQ to 160	49	100	18 to 29	24	0	–	–	92	<LOQ to 15	8.0
PFDA	0.08	30	<LOQ to 24	4.6	0	–	–	0	–	–	92	<LOQ to 45	14
PFUnDA	0.05	100	18 to 53	32	100	11 to 30	19	80	<LOQ to 7.8	5.3	100	17 to 300	70
PFDoDA	0.02	30	<LOQ to 4.1	1.1	0	–	–	0	–	–	92	<LOQ to 24	7.7
PFTriDA	0.06	60	<LOQ to 18	8.4	0	–	–	40	<LOQ to 6.1	2.4	100	5.8 to 48	22
PFTeDA	0.06	0	–	–	0	–	–	0	–	–	50	<LOQ to 3.7	1.4
PFSAs													
L–PFBS	0.09	0	–	–	0	–	–	0	–	–	0	–	–
L–PFPeS	0.13	0	–	–	0	–	–	0	–	–	0	–	–
L–PFHxS	0.22	0	–	–	0	–	–	0	–	–	0	–	–
br–PFHxSK	0.05	0	–	–	0	–	–	0	–	–	0	–	–
L–PFOS	0.26	0	–	–	0	–	–	0	–	–	0	–	–
br–PFOSK	0.12	30	<LOQ to 28	6.2	0	–	–	0	–	–	58	<LOQ to 7.1	3.2
L–PFHpS	0.12	0	–	–	0	–	–	0	–	–	0	–	–
L–PFNS	0.11	0	–	–	0	–	–	0	–	–	0	–	–
L–PFDS	0.26	0	–	–	0	–	–	0	–	–	0	–	–
Precursors													
N–MeFOSAA	0.17	0	–	–	0	–	–	0	–	–	0	–	–
N–EtFOSAA	0.25	0	–	–	0	–	–	0	–	–	0	–	–
4:2 FTS	0.49	0	–	–	0	–	–	0	–	–	0	–	–
6:2 FTS	0.34	0	–	–	0	–	–	0	–	–	0	–	–
8:2 FTS	0.31	0	–	–	0	–	–	0	–	–	0	–	–
Alternatives													
ADONA	0.05	0	–	–	0	–	–	0	–	–	0	–	–
Gen–X	0.07	0	–	–	0	–	–	0	–	–	0	–	–
F53B	0.15	0	–	–	0	–	–	0	–	–	0	–	–
∑PFASs			64 to 920	300		71 to 170	120		<LOQ to 26	14		30 to 510	150

[a] DR: Detection rate (%).
[b] <LOQ: Below limit of quantification.
[c] –: Below limit of detection.

Louis, MO), which were preconditioned with 3 mL of methanol. The target analytes were eluted by passing 1 mL of the sample concentrate through the cartridge, followed by sequential elution with 4 mL of methanol. The eluate was then concentrated to 1 mL using a nitrogen evaporator under a gentle N_2 gas flow at 40 °C. The final eluate was passed through a 0.2-μm PP filter.

The analysis of 28 PFASs was performed using an Agilent 1290 Infinity II HPLC coupled to a triple quadrupole mass spectrometer (6470, Agilent Technologies, Santa Clara, CA). Separation of the target PFASs was achieved using an ACQUITY UPLC® BEH Shield RP_{18} column (2.1 × 100 mm, 1.7 μm, Waters, Milford, MA) with the column temperature maintained at 30 °C. The mobile phase consisted of (A) water and (B) 80 % methanol in acetonitrile, each containing 10 mM ammonium acetate buffer. The gradient elution condition of the mobile phases is provided in Table S3. The mass spectrometer operated in negative electrospray ionization mode, and analyses were conducted using multiple reaction monitoring. Optimized conditions of the tandem mass spectrometer for analyzing PFASs are summarized in Table S4.

2.4. Quality control

Calibration curves for individual PFASs were established using nine concentration points (0.1–50 ng mL^{-1}), and PFAS concentrations in sediment samples were quantified using an external standard method (Table S5). The coefficient of determination (R^2) for all target compounds exceeded 0.99. To monitor potential background contamination and carryover during instrumental analysis, a 5 ng mL^{-1} standard solution and an instrumental blank (PFAS-free methanol) were analyzed every 10 samples. No interfering peaks were observed in the blanks, indicating the absence of instrument-related contamination. The limits of detection (LOD) and quantitation (LOQ) were defined based on signal-to-noise (S/N) ratios of 3 and 10, respectively, with LOQs ranging from 0.02 to 0.49 ng g^{-1} dry weight. Average recoveries of the internal standards ranged from 68 % to 83 % (Table S6). These validation parameters, including calibration linearity, S/N thresholds, and recovery rates, are consistent with internationally recognized guidelines for chromatographic method validation (Yüksel and Şen, 2018; Yüksel, 2020). In addition, matrix effects were evaluated by comparing PFAS-spiked sediment samples with standard solutions at equivalent concentrations. Minimal signal suppression or enhancement (<15 %) was observed, indicating negligible matrix effects. Selectivity was confirmed by the absence of interfering peaks at the retention times of the target PFASs in both instrumental blanks and matrix-matched standards.

2.5. Statistical analysis

The normality of PFAS concentration data was assessed using the Shapiro–Wilk test in R software (version 4.2.3). As most variables exhibited non-normal distributions, log transformation was applied. After transformation, all variables satisfied the assumption of normality ($p > 0.05$), supporting the appropriateness of parametric statistical methods. Based on normalized data, a one-way ANOVA followed by Tukey's HSD post hoc test was performed to assess spatial differences in PFAS concentrations among the four regional seas. Chi-square tests were conducted to assess changes in the relative proportions of PFASs across sediment depths within each core, and one-way ANOVA was employed to evaluate differences in compound concentrations across sediment depths. PCA was conducted using IBM SPSS Statistics 26 (Armonk, NY) to identify the compositional characteristics and distribution patterns of PFASs in sediments. Bartlett's test and the Kaiser-Meyer-Olkin (KMO) measure were applied to assess the suitability of the data for PCA, with the KMO value exceeding 0.6, indicating adequate sampling adequacy. Additionally, a Kolmogorov-Smirnov test was performed on the dataset used for PCA, yielding a p-value >0.05, confirming that the data followed a normal distribution.

2.6. Calculation of water-sediment partition coefficients of PFASs

The partitioning behavior of PFASs between seawater and sediment was assessed using the field-based partitioning coefficients (K_d, L kg^{-1}). The equation used for this calculation is as follows (Wang et al., 2023) (Eq. (1)).

$$K_d = C_{sediment}/C_{water} \quad (1)$$

where C_s and C_w represent the concentrations of PFASs in sediment (ng kg^{-1}) and bottom seawater (ng L^{-1}), respectively. Concentrations of PFASs in seawater at the same sites of this study were reported previously (Yang et al., 2025).

3. Results and discussion

3.1. OC, TN, and C/N ratios in surface sediments

The OC contents in sediments varied across the studied regions, with ranges of 0.12–0.97 % (mean = 0.58 %) in YS, 0.34–0.68 % (mean = 0.50 %) in ECS, 0.16–1.3 % (mean = 0.95 %) in SS, and 0.21–3.5 % (mean = 2.7 %) in ES (Fig. 2a, Fig. S2, and Table S1). The ES sediments exhibited the highest OC contents, likely due to their fine grain size, consistent with findings from previous studies (Brenan et al., 2024; Kim et al., 2021). In YS, relatively high OC contents were observed at certain sites, likely due to the presence of the Central Yellow Sea Mud Zone influenced by hydrodynamic and oceanographic conditions (Qiao et al., 2017). The TN contents ranged from 0.02 to 0.15 % (mean = 0.09 %) in YS, 0.04–0.20 % (mean = 0.15 %) in ECS, and 0.06–0.11 % (mean = 0.08 %) in SS (Table S1). The C/N ratio, representing the OC to TN ratio, indicates organic matter sources. The C/N ratio is an indicator of organic matter content (OC/TN) and indicates the source of organic matter. The C/N ratio of sediments in the South Korean waters ranges from 3.7 to 7.1, suggesting that organic matter derived from bacteria, algae, and marine productivity are the main contributors (Saibro et al., 2023; Sen and Bhadury, 2017). TN contents for ES were not analyzed, preventing the calculation of the C/N ratio in this region. In addition, $\delta^{13}C$ values were analyzed to further assess the sources of organic matter. $\delta^{13}C$ values of surface sediments ranged from −22.54 ‰ to −20.89 ‰ (Table S1), consistent with organic matter predominantly derived from marine phytoplanktons (typically −22 ‰ to −19 ‰) (Lee et al., 2022; Saibro et al., 2023). These isotopic signatures support the C/N-based inference that sedimentary organic matter is primarily autochthonous. However, because $\delta^{13}C$ data were not measured for surface sediments from ES and $\delta^{15}N$ data were only available at some sites, a comprehensive interpretation using dual-isotope analysis could not be performed across all sampling sites. A significant correlation was observed between PFAS concentrations and OC contents in the sediments ($p < 0.05$) (Fig. S3). In previous studies, the mud content of sediments from the regional seas of Korea was highest in the ES (>90 %), which was significantly higher than in the YS and the SS, and showed a significant positive correlation with the OC content (Kim et al., 2021; Hubert et al., 2023). The regional variations in OC contents across the four seas were influenced mainly by differences in sediment grain size (Brenan et al., 2024). Given these variations, a direct comparison of PFASs contamination based on dry weight may not be appropriate (Kim et al., 2021). Thus, this study normalized PFAS concentrations to OC contents to ensure comparability across regions.

3.2. Spatial distributions of PFASs in surface sediments

Among the 28 PFASs, nine PFCAs and one PFSA were detected in surface sediments from the regional seas of South Korea (Table 1 and Table S7). The total PFAS concentrations ranged from <LOQ to 820 ng g^{-1} OC, with a mean concentration of 170 ng g^{-1} OC. In all sediments, PFCAs were consistently detected at higher concentrations than PFSAs,

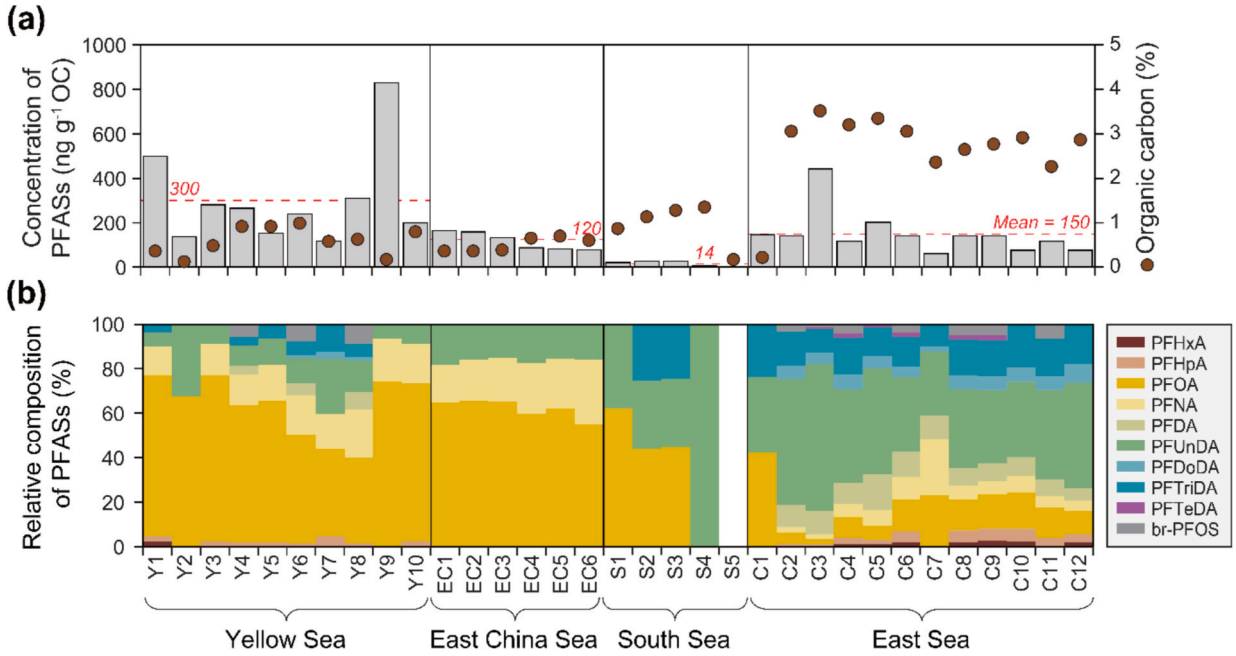

Fig. 2. (a) Spatial distributions of organic carbon (OC) and PFASs, and (b) compositional profiles of PFASs in surface sediments from the Yellow Sea, East China Sea, South Sea, and East Sea. The red dotted lines indicate the mean concentration for each regional sea. (For interpretation of the references to color in this figure legend, the reader is referred to the web version of this article.)

with long-chain PFCAs (C_8–C_{11}) being the dominant compounds. PFUnDA was the most abundant compound, with a mean concentration of 39 ng g^{-1} OC and a detection frequency of 97 %. This was followed by PFOA (mean = 80 ng g^{-1} OC) and PFNA (22 ng g^{-1} OC), which exhibited detection frequencies of 94 % and 79 %, respectively. The detection frequencies of other PFASs were as follows: PFTriDA (11 ng g^{-1} OC, 61 %), PFHpA (2.5 ng g^{-1} OC, 55 %), PFDA (6.4 ng g^{-1} OC, 42 %), PFDoDA (3.1 ng g^{-1} OC, 42 %), br-PFOS (3.0 ng g^{-1} OC, 30 %), PFHxA (0.85 ng g^{-1} OC, 27 %), and PFTeDA (0.52 ng g^{-1} OC, 18 %).

The highest concentrations of PFASs in surface sediments were observed in YS (mean = 300 ng g^{-1} OC), followed by ES (150 ng g^{-1} OC), ECS (120 ng g^{-1} OC), and SS (14 ng g^{-1} OC) (Fig. 2a and Table S1). Statistical analyses revealed significant spatial differences in PFAS concentrations among the four regions. One-way ANOVA, followed by Tukey's HSD test, indicated that concentrations in the YS and ECS were significantly higher than those in the SS and ES for several PFASs, including PFOA, PFNA, and PFUnDA ($p < 0.05$). Detailed statistical results are provided in Table S8. Elevated PFAS concentrations were particularly evident at sites located near the mainland of China and Korea, including Y1, Y3, and Y9 in YS and EC1 in ECS. The concentrations of PFASs in sediments exhibited a gradual decline toward the open sea, a pattern consistent with previous observations in seawater (Gao et al., 2014; Yang et al., 2025). The highest PFASs concentration was found at site Y9, with a value of 960 ng g^{-1} OC. The elevated PFAS levels in this region may be attributed to the transport and accumulation of these contaminants in muddy sediments, influenced by oceanic circulation and hydrodynamic conditions (Li et al., 2015; Lin et al., 2017; Qiao et al., 2017). Additionally, the strong adsorption of hydrophobic chemicals onto fine sediments in mud-dominated areas may further contribute to the observed PFASs accumulation (Hubert et al., 2023).

Notably, site C3 in ES, located in waste dumpsites, exhibited higher PFAS concentrations than other ES sites. PFAS levels generally decreased from the dumping area toward the northeast, a trend also observed at sites C2, C7, C9, and C10. This distribution pattern is likely influenced by the East Korean Warm Current, a northward-flowing branch of the Tsushima Warm Current (TsWC) along the southeastern coast of the Korean Peninsula (Fig. S3) (Kim et al., 2020). Furthermore, previous studies have reported that Sn, among other heavy metals discharged at the ES dumpsite, was transported northeastward by ocean currents and subsequently deposited on the seabed (Um et al., 2024), a trend that aligns with the spatial distribution of PFASs observed in this study.

Overall, the spatial distributions of PFASs in sediments are influenced by ocean currents, vary with sediment grain size, and may be further exacerbated by ocean dumping. The high detection rates of long-chain PFASs in sediments can be attributed to their greater affinity for sediments, which enhances their sorption and persistence (Bai and Son, 2021). Among the long-chain PFAS compounds, PFUnDA was the dominant compound in ES, whereas PFOA was the predominant species in YS, ECS, and SS (Fig. 2b). The presence of PFUnDA in ES sediments may be attributed to the accumulation of long-chain PFASs by the high OC contents in this region. This suggests regional variations in the types of PFASs utilized, potentially reflecting differences in industrial activities and sources. PFAS-related industries, including semiconductor manufacturing, paper mills, and automobile production along the coastal areas of YS, may contribute to the elevated PFOA contamination in this region (Lee et al., 2020a). In the Bohai Sea, which is bordered by highly industrialized provinces such as Tianjin and Shandong, PFOA was the dominant PFAS in both seawater and sediments, accounting for over 48 % of total PFASs. This contamination is largely attributed to the Xiaoqing River, which discharges into Laizhou Bay and receives effluents from fluorochemical and fluoropolymer manufacturing facilities (Meng et al., 2021). In contrast, PFAS concentrations in the Japan Sea are relatively lower, likely due to the limited presence of direct industrial discharges along its coastline. Instead, PFAS inputs are primarily associated with oceanic inflow via the TsWC, which transports contaminants from the ECS and nearby industrialized regions (Yang et al., 2025; Yamazaki et al., 2019).

Although this study did not assess ecological risks, the accumulation of long-chain PFASs in sediments may pose threats to benthic organisms. These organisms inhabit and feed within the sediment matrix and are thus likely to be exposed to sedimentary PFASs (Simpson et al., 2021). PFASs can subsequently bioaccumulate and be transferred through benthic food webs, potentially amplifying their toxic effects (Munoz

et al., 2022; Simpson et al., 2021). These findings highlight the need for future studies to evaluate the bioavailability and ecotoxicity of PFASs to sediment-dwelling organisms.

3.3. Vertical profiles of PFASs in core sediments

A total of 12 PFASs were detected in the core sediments, including 9 PFCAs, 2 PFSAs, and one precursor (Fig. 3 and Table S7). The total PFAS concentrations ranged from <LOQ to 450 ng g^{-1} OC (mean = 41 ng g^{-1} OC). In all core sediments, PFCAs were consistently detected at higher concentrations than PFSA, with long-chain PFCAs being the predominant compounds, a trend similar to that observed in surface sediments. Additionally, as in surface sediments, PFUnDA showed the highest detection frequency (43 %), with a mean concentration of 24 ng g^{-1} OC), followed by PFTriDA (7.1 ng g^{-1} OC, 32 %) and PFDoDA (2.8 ng g^{-1} OC, 27 %). Significant variations in PFAS composition were observed with increasing sediment depth. Chi-square tests for Cores C1, C3, and C10 revealed statistically significant differences in PFAS composition at each core ($p < 0.01$ for all three cores), indicating that PFAS profiles varied substantially with depth at each site. In addition, one-way ANOVA was used to assess variations in PFOA concentrations with sediment depth. The p-value obtained for PFOA ($p = 0.056$) suggested that changes in PFOA concentrations across sediment depths were not statistically significant.

Among the core samples, the highest PFAS concentrations were detected at site C3, a known waste dumpsite, followed by sites C1 and C10. Concentrations were highest in the surface layers and gradually declined with increasing depth. PFAS profiles in the cores were dominated by PFUnDA, indicating its persistence and widespread use over time. Sediment dating using ^{210}Pb revealed a well-mixed upper ~10 cm layer at C3, likely caused by physical disturbances from historical waste dumping activities, while the mixed layer at C1 was comparatively thinner (Hong and Shin, 2009; Um et al., 2024). For both C1 and C3, however, dating results for the upper layers were deemed unreliable due to such disturbances. Consequently, we referred to previously reported data, with the disturbed surface layer at C3 estimated to correspond to sediment deposited around 1990. The use of previously established chronology when direct dating is hindered has been adopted in other marine sediment studies facing similar challenges (Muschitiello et al., 2020).

Geochemical indicators supported these observations: δ^{13}C values in the upper 10 cm of the C3 core were approximately 2 ‰ lighter, and OC contents were higher compared to deeper layers, suggesting the input of exogenous organic matter (Park, 2008; Hong and Shin, 2009). Below 10 cm depth, both δ^{13}C values and OC contents remained stable (Table S9), indicating undisturbed, older sediments. In contrast, the PFAS profiles in the C10 core appeared unaffected by dumped wastes. Instead, PFAS concentrations increased markedly from the 1950s onward, coinciding with the global onset of PFAS production and use. The highest concentrations were observed in the most recent sediment layers, reflecting regional and global consumption trends (Shen et al., 2018; Wang et al., 2025).

3.4. Principal component analysis of sedimentary PFASs across sampling sites

PCA was used to characterize the spatial distribution patterns of PFASs in sediments of the regional seas of Korea. PC1 accounted for 49.9 % of the total variance, and PC2 accounted for 31.5 %, together explaining 81.4 % of the total variance. The sampling sites were grouped into three distinct clusters based on the PFAS compositions (Fig. 4a and Table S10). To validate the grouping of sampling sites into three distinct clusters, the factor loadings for PC1 and PC2 are presented in Table S11. Group 1 was characterized by PFOA and PFNA, predominantly found in sediments from the YS and ECS (Fig. 4b). This distribution pattern aligns with previous findings from the YS and ECS (Zhong et al., 2021). The

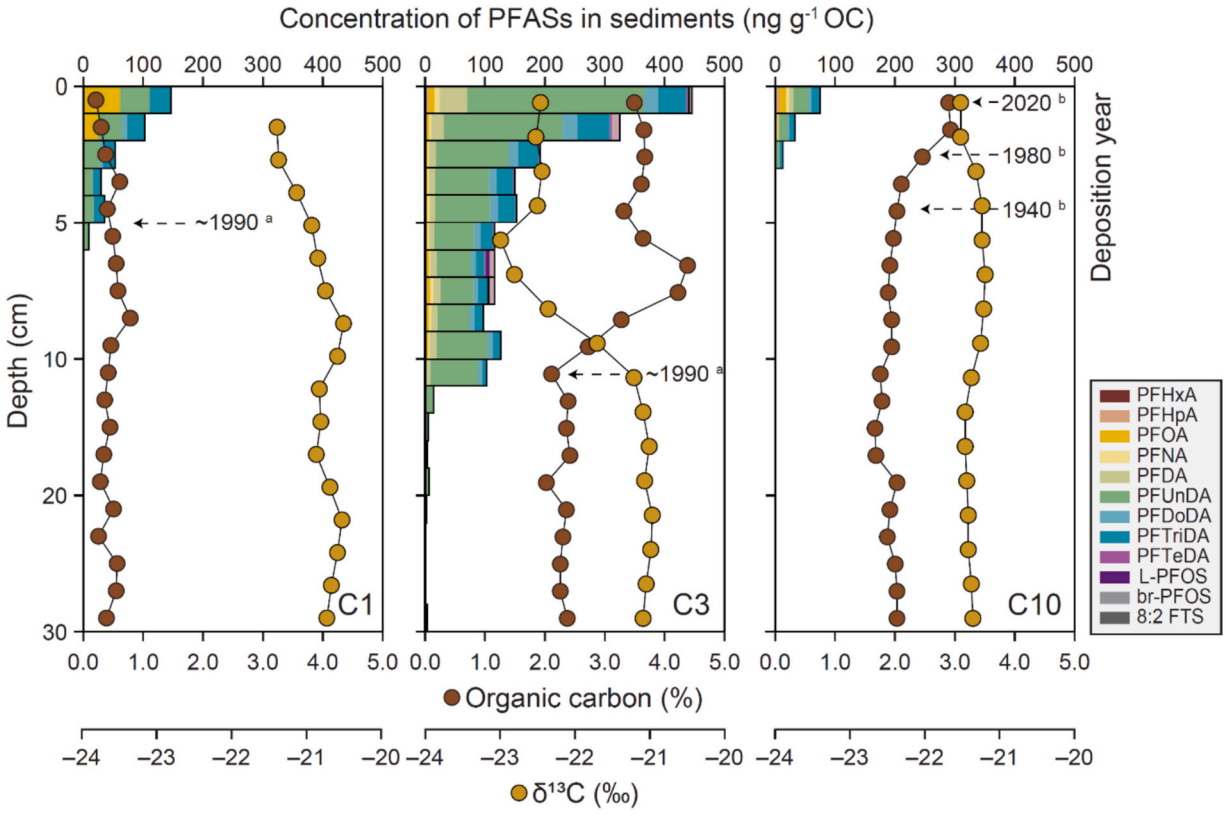

Fig. 3. Vertical distributions of PFASs, organic carbon (OC), and carbon stable isotope ratios (δ^{13}C) in core sediments from sites C1, C3, and C10. Sediment chronology at similar locations was reported in previous studies ([a] Hong and Shin, 2009; [b] Um et al., 2024).

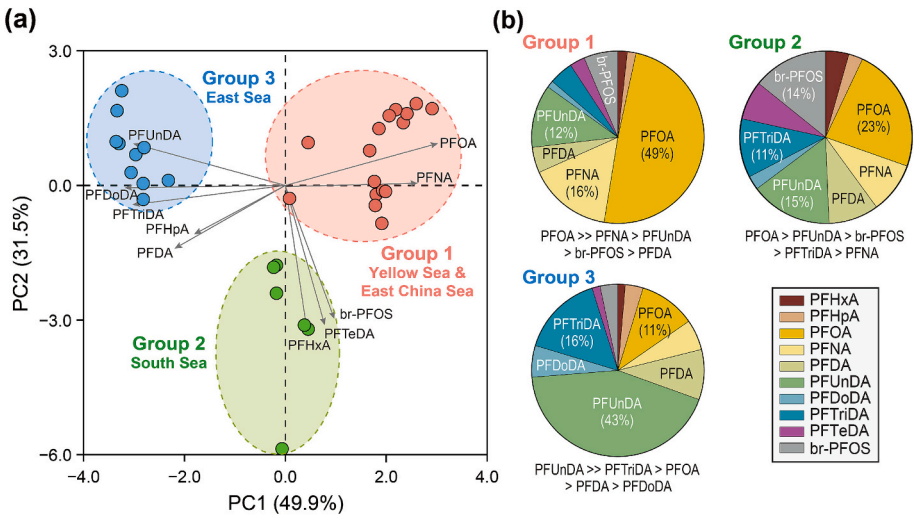

Fig. 4. (a) Principal component analysis (PCA) results for PFAS compositions in surface sediments from the regional seas of South Korea. (b) Relative compositions of PFASs in each group based on PCA classification (Group 1: Yellow Sea and East China Sea; Group 2: South Sea; Group 3: East Sea).

major sources of PFOA and PFNA in this region are attributed to fluoropolymer production, particularly the manufacturing of polytetrafluoroethylene and polyvinylidene fluoride in fluorination plants along the lower reaches of the Yangtze River (CAFSI, 2019). The presence of these compounds suggests that inflow from the Yangtze River exerts a significant influence on PFASs distribution in this cluster (Du et al., 2022). A significant positive correlation ($p < 0.05$) was observed between OC and PFNA concentrations in the YS, consistent with previous studies demonstrating the strong influence of OC on the adsorption of long-chain PFASs (Fig. S3) (Li et al., 2024b). However, no significant correlation was found between OC and either PFOA or PFNA in the ECS, indicating that OC was not a major factor controlling PFASs distribution in ECS (Li et al., 2024b).

Group 2 was characterized by PFHxA, PFTeDA, and br-PFOS, with these compounds predominantly detected at sites in the SS (Fig. 4a). Previous studies have reported frequent detection of PFHxA, PFTeDA, and PFOS in the YS and ECS, with PFHxA specifically identified as a replacement for PFOA following its recent regulatory restrictions in Jiangsu Province (Zhong et al., 2021). Water masses from the ECS continental shelf are likely transported via the TsWC toward the SS, where these compounds subsequently accumulate in the sediments (Fig. S4) (Kodama et al., 2015). These findings further support the observed shift in PFAS consumption patterns, with increasing reliance on alternative substances due to the regulation of long-chain PFASs (Du et al., 2022). Group 3 was distinguished by a combination of both short- and long-chain PFASs, including PFHpA, PFDA, PFUnDA, PFDoDA, and PFTriDA, with sites in the ES falling into this cluster (Fig. 4a). Among these compounds, PFDA, PFUnDA, PFDoDA, and PFTriDA exhibited significant positive correlations with OC. The relatively high OC content in ES sediments compared to those in the YS, ECS, and SS likely enhances the adsorption of PFASs onto sediment particles (Oliver et al., 2020).

Overall, the PCA results indicate that the distribution of PFASs in sediments is influenced by multiple factors, including source inputs, OC content, and transport via ocean currents. Variations in the dominant PFAS composition among groups likely reflect differences in the types of PFAS used near the sampling locations. Additionally, the adsorption behavior of PFASs appears to be influenced by OC content at individual sites (Li et al., 2024b). However, the adsorption mechanisms of PFASs in the environment are complex and cannot be explained solely by OC content (Li et al., 2018c). Given that PFASs are highly mobile and can be transported over long distances via ocean currents, these currents may represent a key factor in determining the composition and spatial distribution of PFASs in sediments (Feng et al., 2020; Gao et al., 2014).

3.5. Water-sediment partitioning behavior of PFASs

In this study, we compared the compositional profiles of PFASs in seawater and sediments in the regional seas of South Korea. A previous study by Yang et al. (2025) analyzed seawater samples collected from the surface at the same (YS, ECS, and SS) or similar (ES) sampling sites as those in the present study. The composition profiles of PFAS compounds exhibited significant differences between seawater and sediments, with PFCAs contributing more substantially than PFSAs. In seawater samples, PFOA was consistently the dominant compound across all sites, accounting for 71 %, 69 %, 67 %, and 70 % of the total PFASs composition in YS, ECS, SS, and ES, respectively (Yang et al., 2025). PFOA is primarily discharged from the Yangtze River at an estimated annual rate of 26.8 tons, contributing to over 80 % of total PFAS emissions in coastal areas (Du et al., 2022). In addition to PFOA, short-chain PFAS compounds such as PFBA, PFPeA, PFHxA, PFHpA, and L-PFBS were predominant in seawater samples. These short-chain PFASs exhibit higher hydrophilicity in aquatic environments compared to long-chain PFASs, enabling their long-range transport via ocean currents persistence (Li et al., 2018a; Shi et al., 2015; Wang et al., 2016).

In sediment samples, long-chain PFASs were predominantly detected compared to short-chain PFASs, likely due to their lower water solubility and stronger adsorption affinity for sediment particles (Table S7) (Kucharzyk et al., 2017; Lee et al., 2020b). PFOA and PFUnDA were the dominant compounds in sediments, showing regional variations. PFOA accounted for 61 %, 63 %, 47 %, and 12 % of the total PFASs composition in the sediments of the YS, ECS, SS, and ES, respectively. The highest proportion of PFOA was observed in the YS, consistent with previous studies (Lee et al., 2020a). The gradual decline in PFOA composition from YS to ES may reflect dilution effects driven by ocean currents and the compound-specific partitioning behavior between water and particulate matter (Wang et al., 2019). PFUnDA contributed 11 %, 16 %, 36 %, and 47 % of the PFAS composition in YS, ECS, SS, and ES sediments, respectively. Other long-chain PFASs, including PFNA, PFDoDA, PFTriDA, and PFTeDA, were also detected, likely due to their strong affinity for sediments (Bai and Son, 2021).

In this study, K_d for four PFASs, such as PFHxA, PFHpA, PFOA, and PFNA, were determined in the regional seas of Korea to investigate their transport and fate characteristics (Fig. 5). The average log K_d values for PFHxA, PFHpA, PFOA, and PFNA were 0.71, 1.6, 2.2, and 1.0, respectively, which are consistent with values reported in the previous study (Lee et al., 2020a). Among the four regional seas, the highest K_d values were observed in the following order: ES > YS > ECS > SS. The regional

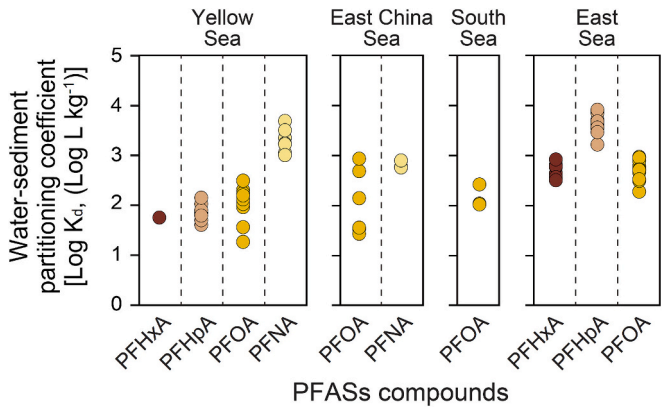

Fig. 5. Field-based water-sediment partitioning coefficients (log K_d) of PFASs in the Yellow Sea, East China Sea, South Sea, and East Sea. Concentrations of PFASs in bottom water samples were previously reported (Yang et al., 2025).

variations in K_d values for PFASs may be attributed to (1) decreased aqueous-phase concentrations as the substances disperse from their source and (2) enhanced adsorption onto sediments due to increased OC content. Additionally, the K_d values generally increased with the carbon chain length of PFASs, corroborating findings from previous research (Liu et al., 2019). These results suggest that the number of carbon atoms is a key factor influencing the partitioning behavior of PFASs between seawater and sediments.

The K_d values of long-chain PFASs obtained in this study were compared with those reported for lakes, rivers, coastal waters, and regional seas (Table S12). The log K_d values exhibited a positive correlation with carbon chain length, with values in coastal and regional seas being comparable to or higher than those observed in lakes and rivers. For instance, the mean log K_d of PFHxA was reported as 0.76 in Poyang Lake, 1.7 in Korean coastal waters, and 3.58 in the Bohai Sea (Lee et al., 2020a; Zhao et al., 2020; Tang et al., 2022). In freshwater environments such as lakes and rivers, PFAS concentrations tend to be higher in the aqueous phase due to direct point-source discharges. In contrast, dilution by ocean currents in coastal areas leads to lower water-phase concentrations and correspondingly log K_d values (Wang et al., 2019). Additionally, variations in log K_d values are influenced by sediment characteristics and salinity (Uchida and Tagami, 2017). In this study, salinity increased progressively from the YS to the ECS, SS, and ES, which likely contributed to the enhanced adsorption of long-chain PFASs in the ES. These differences illustrate that PFASs, especially long-chain compounds, tend to exhibit stronger sediment-water partitioning in marine environments than in freshwater systems, as evidenced by generally higher log K_d values reported for coastal and regional seas worldwide. This trend is likely driven by a combination of lower aqueous concentrations due to dilution, higher ionic strength, and enhanced sorption under saline conditions.

3.6. Comparison of sedimentary PFASs in rivers, estuaries, and regional seas

The concentrations of identified PFASs in sediments from the seas surrounding Korea were compared with those reported in sediments from adjacent rivers and marine environments (Table S13). The PFAS concentrations in sediments from the YS were comparable to those observed in the Bohai Sea and the Yangtze River Estuary (Zhao et al., 2020; Li et al., 2024a). Similarly, the concentrations of sedimentary PFASs in the ECS were consistent with previously reported values for the region (Gao et al., 2014). In contrast, PFAS concentrations in sediments from the SS were lower than those reported in the Bohai Sea, the Yangtze River Estuary, the Korean coastal region, and rivers in Korea (Gao et al., 2014; Lam et al., 2014; Lee et al., 2020a; Zhao et al., 2020; Li et al., 2024a). The SS is influenced by the Tsushima Current, a branch of the Kuroshio Warm Current, which likely contributes to substantial dilution of PFASs, resulting in reduced sedimentary concentrations (Kodama et al., 2015; Wang et al., 2019). Conversely, PFAS concentrations detected in surface sediments from the ES exceeded those reported in sediments from surrounding rivers and marine areas. This trend may be attributed to the enhanced adsorption of PFASs onto sediments in the ES, which is associated with finer grain sizes and high OC contents (Brenan et al., 2024; Hubert et al., 2023; Kim et al., 2021).

PFOA and br-PFOS were identified as the predominant PFASs in the sediments of the Bohai Sea, Yangtze River Estuary, YS, and ECS (Fig. S5) (Zhao et al., 2020; Li et al., 2024a; Zhu et al., 2025). This finding suggests that, despite regulatory measures, these compounds continue to be emitted and accumulated into the marine environment. Studies conducted following the implementation of PFAS regulations indicate that while PFOA remains the dominant compound, the detection of short-chain PFASs, such as PFHxA and PFHpA, has increased (Zhao et al., 2020; Li et al., 2024a; Zhu et al., 2025). This trend likely reflects a shift in PFASs production and consumption patterns toward short-chain alternatives.

4. Conclusion

This study examined the distribution and compositional characteristics of 28 PFASs in sediments from regional seas surrounding South Korea. Despite global regulatory efforts, PFOA remains prevalent in South Korean coastal waters. The highest concentrations in core sediments were observed in recent years, indicating a gradual increase in usage. The spatial distribution of PFASs suggests that ocean currents and regional variations in sediment grain size may influence their transport and deposition. As this study primarily focused on the distribution and composition of PFASs in sediments, further research is needed to assess the ecological risks to aquatic organisms and humans and identify additional sources and transport of contamination. The findings of this study contribute to a more comprehensive understanding of PFAS contamination in the regional seas, and can serve as a foundation for developing effective contamination management and mitigation strategies.

CRediT authorship contribution statement

Sunmi Yang: Writing – original draft, Visualization, Investigation, Formal analysis, Data curation, Conceptualization. **Jiyun Gwak:** Visualization, Investigation, Formal analysis. **Jihyun Cha:** Visualization, Formal analysis. **Kiho Park:** Investigation, Formal analysis. **Youngnam Kim:** Investigation, Formal analysis. **Sea-Yong Kim:** Visualization, Formal analysis. **Yeonjung Lee:** Investigation, Formal analysis. **Dong Han Choi:** Project administration, Investigation, Formal analysis. **Kongtae Ra:** Investigation, Formal analysis. **Hyo-Bang Moon:** Writing – review & editing, Methodology, Formal analysis, Data curation. **Seongjin Hong:** Writing – review & editing, Visualization, Supervision, Project administration, Investigation, Funding acquisition, Formal analysis, Conceptualization.

Declaration of competing interest

The authors declare that they have no known competing financial interests or personal relationships that could have appeared to influence the work reported in this paper.

The author is an Editorial Board Member/Editor-in-Chief/Associate Editor/Guest Editor for this journal and was not involved in the editorial review or the decision to publish this article.

Acknowledgments

This work was supported by grants from the National Research

Foundation of Korea (NRF) (2022R1A4A1033825) and the Korea Institute of Marine Science & Technology Promotion (KIMST) funded by the Ministry of Oceans and Fisheries (2021-0696, RS-2023-00256330, and RS-2024-00417889).

Appendix A. Supplementary data

Supplementary data to this article can be found online at https://doi.org/10.1016/j.marpolbul.2025.118140.

Data availability

Data will be made available on request.

References

Bai, X., Son, Y., 2021. Perfluoroalkyl substances (PFAS) in surface water and sediments from two urban watersheds in Nevada, USA. Sci. Total Environ. 751, 141622. https://doi.org/10.1016/j.scitotenv.2020.141622.

Brenan, C., Kienast, M., Maselli, V., Algar, C.K., Misiuk, B., Brown, C.J., 2024. Seafloor sediment characterization improves estimates of organic carbon standing stocks: an example from the eastern shore islands, Nova Scotia, Canada. Biogeosciences 21, 4569–4586. https://doi.org/10.5194/bg–21–4569–2024.

CAFSI, 2019. White Paper on the Development of Chinese Fluorochemical Industry. China Association of Fluorine and Silicone Industry (CAFSI), Beijing (in Chinese).

Chung, C.S., Choi, K.-Y., Kim, C.-J., Jung, J.-M., Chang, Y.S., 2020. Overview of the policies for phasing out ocean dumping of sewage sludge in the Republic of Korea. Sustainability 12, 4553. https://doi.org/10.3390/su12114553.

D'Eon, J.C., Mabury, S.A., 2011. Is indirect exposure a significant contributor to the burden of perfluorinated acids observed in humans? Environ. Sci. Technol. 45, 7974–7984. https://doi.org/10.1021/es200171y.

Diao, J., Chen, Z., Wang, T., Su, C., Sun, Q., Guo, Y., Zheng, Z., Wang, L., Li, P., Liu, W., Hong, S., Khim, J.S., 2022. Perfluoroalkyl substances in marine food webs from South China Sea: trophic transfer and human exposure implication. J. Hazard. Mater. 431, 128602. https://doi.org/10.1016/j.jhazmat.2022.128602.

Du, D., Lu, Y., Zhou, Y., Zhang, M., Wang, C., Yu, M., Song, S., Cui, H., Chen, C., 2022. Perfluoroalkyl acids (PFAAs) in water along the entire coastal line of China: spatial distribution, mass loadings, and worldwide comparisons. Environ. Int. 169, 107506. https://doi.org/10.1016/j.envint.2022.107506.

Eo, S., Hong, S.H., Song, Y.K., Han, G.M., Seo, S., Park, Y.-G., Shim, W.J., 2022. Underwater hidden microplastic hotspots: historical ocean dumping sites. Water Res. 216, 118254. https://doi.org/10.1016/j.watres.2022.118254.

Feng, X., Ye, M., Li, Y., Zhou, J., Sun, B., Zhu, Y., Zhu, L., 2020. Potential sources and sediment-pore water partitioning behaviors of emerging per/polyfluoroalkyl substances in the South Yellow Sea. J. Hazard. Mater. 389, 122124. https://doi.org/10.1016/j.jhazmat.2020.122124.

Gao, Y., Fu, J., Zeng, L., Li, A., Li, H., Zhu, N., Liu, R., Liu, A., Wang, Y., Jiang, G., 2014. Occurrence and fate of perfluoroalkyl substances in marine sediments from the Chinese Bohai Sea, Yellow Sea, and East China Sea. Environ. Pollut. 194, 60–68. https://doi.org/10.1016/j.envpol.2014.07.018.

Hong, S., Shin, K.H., 2009. Alkylphenols in the core sediment of a waste dumpsite in the East Sea (Sea of Japan), Korea. Mar. Pollut. Bull. 58, 1566–1571. https://doi.org/10.1016/j.marpolbul.2009.07.016.

Hu, J.-J., Yu, S.-K., Yin, C., Peng, F.-J., Liu, S.-S., Pan, C.-G., Yu, K., 2025. Sorption and mechanisms of legacy and emerging per- and polyfluoroalkyl substances (PFASs) on different particle size fractions of marine sediments. Environ. Res. 278, 121643. https://doi.org/10.1016/j.envres.2025.121643.

Hubert, M., Arp, H.P.H., Hansen, M.C., Castro, G., Meyn, T., Asimakopoulos, A.G., Hale, S.E., 2023. Influence of grain size, organic carbon and organic matter residue content on the sorption of per- and polyfluoroalkyl substances in aqueous film forming foam contaminated soils - implications for remediation using soil washing. Sci. Total Environ. 875, 162668. https://doi.org/10.1016/j.scitotenv.2023.162668.

Jiang, L., Huang, Z., Xu, J., Zhang, L., Du, Z., 2024. Selective adsorption of OBS (sodium p-perfluorous nonenoxybenzenesulfonate) as an emerging PFAS contaminant from aquatic environments by fluorinated MOFs: novel mechanisms of F–F exclusive attraction. Chem. Eng. J. 484, 149355. https://doi.org/10.1016/j.cej.2024.149355.

Jung, J.-M., Kim, C.-J., Chung, C.-S., Kim, T., Choi, K.-Y., 2023. Heavy metal characterization of land-based waste dumped at three ocean dumping sites in the Republic of Korea. Mar. Pollut. Bull. 193, 115205. https://doi.org/10.1016/j.marpolbul.2023.115205.

Kennicutt, M., 2017. In: Ward, C.H. (Ed.), Habitats and Biota of the Gulf of Mexico: Before the Deepwater Horizon Oil Spill. Springer Sci. Rev, New York, NY.

Kim, D., Kim, J.-H., Kim, M.-S., Ra, K., Shin, K.-H., 2018. Assessing environmental changes in Lake Shihwa, South Korea, based on distributions and stable carbon isotopic compositions of n-alkanes. Environ. Pollut. 240, 105–115. https://doi.org/10.1016/j.envpol.2018.04.098.

Kim, D., Shin, H.-R., Kim, C.-H., Hirose, N., 2020. Characteristics of the East Sea (Japan Sea) circulation depending on surface heat flux and its effect on branching of the Tsushima Warm Current. Cont. Shelf Res. 192, 104025. https://doi.org/10.1016/j.csr.2019.104025.

Kim, Y., Hong, S., Lee, J., Yoon, S.J., An, Y., Kim, M.-S., Jeong, H.-D., Khim, J.S., 2021. Spatial distribution and source identification of traditional and emerging persistent toxic substances in the offshore sediment of South Korea. Sci. Total Environ. 789, 147996. https://doi.org/10.1016/j.scitotenv.2021.147996.

Kodama, T., Setou, T., Masujima, M., Okazaki, M., Ichikawa, T., 2015. Intrusions of excess nitrate in the Kuroshio subsurface layer. Cont. Shelf Res. 110, 191–200. https://doi.org/10.1016/j.csr.2015.10.012.

Kucharzyk, K.H., Darlington, R., Benotti, M., Deeb, R., Hawley, E., 2017. Novel treatment technologies for PFAS compounds: a critical review. J. Environ. Manage. 204, 757–764. https://doi.org/10.1016/j.jenvman.2017.08.016.

Lam, N.-H., Cho, C.-R., Lee, J.-S., Soh, H.-Y., Lee, B.-C., Lee, J.-A., Tatarozako, N., Sasaki, K., Saito, N., Iwabuchi, K., Kannan, K., Cho, H.-S., 2014. Perfluorinated alkyl substances in water, sediment, plankton and fish from Korean rivers and lakes: a nationwide survey. Sci. Total Environ. 491–492, 154–162. https://doi.org/10.1016/j.scitotenv.2014.01.045.

Lee, J.-W., Lee, H.-K., Lim, J.-E., Moon, H.-B., 2020a. Legacy and emerging per- and polyfluoroalkyl substances (PFASs) in the coastal environment of Korea: occurrence, spatial distribution, and bioaccumulation potential. Chemosphere 251, 126633. https://doi.org/10.1016/j.chemosphere.2020.126633.

Lee, Y.-M., Lee, J.-Y., Kim, M.-K., Yang, H., Lee, J.-E., Son, Y., Kho, Y., Choi, K., Zoh, K.-D., 2020b. Concentration and distribution of per- and polyfluoroalkyl substances (PFAS) in the Asan Lake area of South Korea. J. Hazard. Mater. 381, 120909. https://doi.org/10.1016/j.jhazmat.2019.120909.

Lee, Y., Choi, D.H., Lee, H., Hyun, M.J., Kim, G., Lee, H., Yang, W., Kim, J., Won, J., Ra, K., Jeong, H., Choi, J.Y., Lee, S., Kim, M., Noh, J.-H., 2022. Changes in the characteristics of organic matter associated with hydrodynamics and phytoplankton size structure in the central-eastern Yellow Sea. Sci. Total Environ. 807, 151781. https://doi.org/10.1016/j.scitotenv.2021.151781.

Li, J., Dong, H., Zhang, D., Han, B., Zhu, C., Liu, S., Liu, X., Ma, Q., Li, X., 2015. Sources and ecological risk assessment of PAHs in surface sediments from Bohai Sea and northern part of the Yellow Sea, China. Mar. Pollut. Bull. 96, 485–490. https://doi.org/10.1016/j.marpolbul.2015.05.002.

Li, L., Zheng, H., Wang, T., Cai, M., Wang, P., 2018a. Perfluoroalkyl acids in surface seawater from the North Pacific to the Arctic Ocean: contamination, distribution and transportation. Environ. Pollut. 238, 168–176. https://doi.org/10.1016/j.envpol.2018.03.018.

Li, L., Dong, Y., Qian, G., Hu, X., Ye, L., 2018b. Performance and microbial community analysis of bio-electrocoagulation on simultaneous nitrification and denitrification in submerged membrane bioreactor at limited dissolved oxygen. Bioresour. Technol. 258, 168–176. https://doi.org/10.1016/j.biortech.2018.02.121.

Li, Y., Oliver, D.P., Kookana, R.S., 2018c. A critical analysis of published data to discern the role of soil and sediment properties in determining sorption of per and polyfluoroalkyl substances (PFASs). Sci. Total Environ. 628, 110–120. https://doi.org/10.1016/j.scitotenv.2018.01.167.

Li, L., Han, T., Li, B., Bai, P., Tang, X., Zhao, Y., 2024a. Distribution control and environmental fate of PFAS in the offshore region adjacent to the Yangtze River estuary – a study combining multiple phases analysis. Environ. Sci. Technol. 58, 15779–15789. https://doi.org/10.1021/acs.est.4c03985.

Li, Q., Liu, C., Wang, S., Liu, Y., Ma, X., Li, Y., Li, W., Wang, X., 2024b. Decade-long historical shifts in legacy and emerging per- and polyfluoroalkyl substances (PFAS) in surface sediments of China's marginal seas: ongoing production and ecological risks. Environ. Res. 263, 119978. https://doi.org/10.1016/j.envres.2024.119978.

Lin, Y., Deng, W., Li, S., Li, J., Wang, G., Zhang, D., Li, X., 2017. Congener profiles, distribution, sources and ecological risk of parent and alkyl-PAHs in surface sediments of Southern Yellow Sea, China. Sci. Total Environ. 580, 1309–1317. https://doi.org/10.1016/j.scitotenv.2016.12.094.

Liu, Y., Zhang, Y., Li, J., Wu, N., Li, W., Niu, Z., 2019. Distribution, partitioning behavior and positive matrix factorization-based source analysis of legacy and emerging polyfluorinated alkyl substances in the dissolved phase, surface sediment and suspended particulate matter around coastal areas of Bohai Bay, China. Environ. Pollut. 246, 34–44. https://doi.org/10.1016/j.envpol.2018.11.113.

Meng, L., Song, B., Zhong, H., Ma, X., Wang, Y., Ma, D., Lu, Y., Gao, W., Wang, Y., Jiang, G., 2021. Legacy and emerging per- and polyfluoroalkyl substances (PFAS) in the Bohai Sea and its inflow rivers. Environ. Int. 156, 106735. https://doi.org/10.1016/j.envint.2021.106735.

MOF, 2015. Establishment of a Comprehensive Management System for the Disposal of Waste Materials (XII). Ministry of Oceans and Fisheries (MOF). Final report.

Munoz, G., Liu, J., Vo Duy, S., Sauvé, S., 2019. Analysis of F-53B, Gen-X, ADONA, and emerging fluoroalkylether substances in environmental and biomonitoring samples: a review. Trends Environ. Anal. Chem. 23, e00066. https://doi.org/10.1016/j.teac.2019.e00066.

Munoz, G., Mercier, L., Duy, S.V., Liu, J., Sauvé, S., Houde, M., 2022. Bioaccumulation and trophic magnification of emerging and legacy per-and polyfluoroalkyl substances (PFAS) in a St. Lawrence River food web. Environ. Pollut. 309, 119739. https://doi.org/10.1016/j.envpol.2022.119739.

Muschitiello, F., O'Regan, M., Martens, J., West, G., Gustafsson, Ö., Jakobsson, M., 2020. A new 30 000-year chronology for rapidly deposited sediments on the Lomonosov Ridge using bulk radiocarbon dating and probabilistic stratigraphic alignment. Geochronology 2, 81–91. https://doi.org/10.5194/gchron-2-81–2020.

Mussabek, D., Persson, K.M., Berndtsson, R., Ahrens, L., Nakagawa, K., Imura, T., 2020. Impact of the sediment organic vs. mineral content on distribution of the per-and polyfluoroalkyl substances (PFAS) in lake sediment. Int. J. Environ. Res. Public Health 17, 5642. https://doi.org/10.3390/ijerph17165642.

Oliver, D.P., Navarro, D.A., Baldock, J., Simpson, S.L., Kookana, R.S., 2020. Sorption behaviour of per- and polyfluoroalkyl substances (PFASs) as affected by the

properties of coastal estuarine sediments. Sci. Total Environ. 720, 137263. https://doi.org/10.1016/j.scitotenv.2020.137263.
Park, J.-J., 2008. The applicability of stable isotope analyses on sediments to reconstruct Korean paleoclimate. J. Korean Geogr. Soc. 43, 477–494.
Qiao, S., Shi, X., Wang, G., Zhou, L., Hu, B., Hu, L., Yang, G., Liu, Y., Yao, Z., Liu, S., 2017. Sediment accumulation and budget in the Bohai Sea, Yellow Sea and East China Sea. Mar. Geol. 390, 270–281. https://doi.org/10.1016/j.margeo.2017.06.004.
Saibro, M.B., Martins, M.V.A., Guerra, J.V., Figueira, R.C.L., de Castro Figueiredo Simões, F., Dadalto, T.P., Trevizani, T.H., de Lima Ferreira, P.A., Silva, C.G., dos Reis, A.T., 2023. Transfer of industrial contaminants from the inner to the outer region of Sepetiba Bay (SE Brazil) by dredge spoil dumping activities: a temporal record. Environ. Earth Sci. 82, 560. https://doi.org/10.1007/s12665–023–11259–6.
Sen, A., Bhadury, P., 2017. Intertidal foraminifera and stable isotope geochemistry from world's largest mangrove, Sundarbans: assessing a multiproxy approach for studying changes in sea-level. Estuarine, Coast. Shelf Sci. 192, 128–136. https://doi.org/10.1016/j.ecss.2017.05.010.
Shen, A., Lee, S., Ra, K., Suk, D., Moon, H.-B., 2018. Historical trends of perfluoroalkyl substances (PFASs) in dated sediments from semi-enclosed bays of Korea. Mar. Pollut. Bull. 128, 287–294. https://doi.org/10.1016/j.marpolbul.2018.01.039.
Shi, Y., Vestergren, R., Xu, L., Song, X., Niu, X., Zhang, C., Cai, Y., 2015. Characterizing direct emissions of perfluoroalkyl substances from ongoing fluoropolymer production sources: a spatial trend study of Xiaoqing River, China. Environ. Pollut. 206, 104–112. https://doi.org/10.1016/j.envpol.2015.06.035.
Simpson, S.L., Liu, Y., Spadaro, D.A., Wang, X., Kookana, R.S., Batley, G.E., 2021. Chronic effects and thresholds for estuarine and marine benthic organism exposure to perfluorooctane sulfonic acid (PFOS)-contaminated sediments: influence of organic carbon and exposure routes. Sci. Total Environ. 776, 146008. https://doi.org/10.1016/j.scitotenv.2021.146008.
Tang, A., Zhang, X., Li, R., Tu, W., Guo, H., Zhang, Y., Li, Z., Liu, Y., Mai, B., 2022. Spatiotemporal distribution, partitioning behavior and flux of per- and polyfluoroalkyl substances in surface water and sediment from Poyang Lake, China. Chemosphere 295, 133855. https://doi.org/10.1016/j.chemosphere.2022.133855.
Uchida, S., Tagami, K., 2017. Comparison of coastal area sediment-seawater distribution coefficients (Kd) of stable and radioactive Sr and Cs. Appl. Geochem. 85, 148–153. https://doi.org/10.1016/j.apgeochem.2016.12.023.
Um, I.K., Choi, M.S., Han, S.Y., Choi, S., Yang, D., 2024. Revisiting elemental geochemistry in surface sediments of the Ulleung Basin, East/Japan Sea: signals from ocean dumping materials. Mar. Pollut. Bull. 206, 116747. https://doi.org/10.1016/j.marpolbul.2024.116747.
UNEP, 2010. An Introduction to the Nine Chemicals Added to Stockholm (Convention. Conference of the parties at its fourth meeting).
UNEP, 2019. Decision SC-9/12: listing of perfluorooctanoic acid (2019), its salts and PFOA-related compounds. In: UN Environment, Conference of the Parties to the Stockholm Convention on Persistent Organic Pollutants. SC-9/12.
Wang, Z., Cousins, I.T., Scheringer, M., Hungerbuehler, K., 2015. Hazard assessment of fluorinated alternatives to long-chain perfluoroalkyl acids (PFAAs) and their precursors: status quo, ongoing challenges and possible solutions. Environ. Int. 75, 172–179. https://doi.org/10.1016/j.envint.2014.11.013.
Wang, P., Lu, Y., Wang, T., Meng, J., Li, Q., Zhu, Z., Sun, Y., Wang, R., Giesy, J.P., 2016. Shifts in production of perfluoroalkyl acids affect emissions and concentrations in the environment of the Xiaoqing River basin, China. J. Hazard. Mater. 307, 55–63. https://doi.org/10.1016/j.jhazmat.2015.12.059.
Wang, Q., Tsui, M.M.P., Ruan, Y., Lin, H., Zhao, Z., Ku, J.P.H., Sun, H., Lam, P.K.S., 2019. Occurrence and distribution of per- and polyfluoroalkyl substances (PFASs) in the seawater and sediment of the South China sea coastal region. Chemosphere 231, 468–477. https://doi.org/10.1016/j.chemosphere.2019.05.162.
Wang, S., Lin, X., Li, Q., Li, Y., Yamazaki, E., Yamashita, N., Wang, X., 2022. Particle size distribution, wet deposition and scavenging effect of per- and polyfluoroalkyl substances (PFASs) in the atmosphere from a subtropical city of China. Sci. Total Environ. 823, 153528. https://doi.org/10.1016/j.scitotenv.2022.153528.
Wang, J., Chen, L., Song, Y., Li, Y., Liu, G., Yin, Y., Cai, Y., 2023. Adsorption and environmental behavior of mercury on the sediment from the Yellow Sea of China. J. Hazard. Mater. 443, 130333. https://doi.org/10.1016/j.jhazmat.2022.130333.
Wang, Q., Ruan, Y., Shao, Y., Jin, L., Xie, N., Yang, X., Hong, Y., Wang, H., Tsujimoto, A., Yasuhara, M., Leung, K.M.Y., Lam, P.K.S., 2025. Spatiotemporal trend of PFAS in estuarine sediments: insights into chlorinated polyfluoroalkyl ether sulfonate transformation. Environ. Sci. Technol. 59, 7377–7388. https://pubs.acs.org/doi/10.1021/acs.est.5c02731.
Yamazaki, E., Taniyasu, S., Ruan, Y., Wang, Q., Petrick, G., Tanhua, T., Gamo, T., Wang, X., Lam, P.K., Yamashita, N., 2019. Vertical distribution of perfluoroalkyl substances in water columns around the Japan sea and the Mediterranean Sea. Chemosphere 231, 487–494. https://doi.org/10.1016/j.chemosphere.2019.05.132.
Yang, S., Gwak, J., Kim, M., Cha, J., Kim, Y., Lee, Y., Moon, H.-B., Hong, S., 2025. Spatial and vertical distribution of per- and polyfluoroalkyl substances (PFASs) in the water columns of the regional seas of South Korea. Chemosphere 370, 144042. https://doi.org/10.1016/j.chemosphere.2024.144042.
Yüksel, B., 2020. Quantitative GC-FID analysis of heroin for seized drugs. Ann. Clin. Anal. Med. 11, 38–42. https://doi.org/10.4328/JCAM.6139.
Yüksel, B., Şen, N., 2018. Development and validation of a GC-FID method for determination of cocaine in illicit drug samples. MARMARA Pharm. J. J 22, 511–518. https://doi.org/10.12991/jrp.2018.92.
Zhao, Z., Cheng, X., Hua, X., Jiang, B., Tian, C., Tang, J., Li, Q., Sun, H., Lin, T., Liao, Y., Zhang, G., 2020. Emerging and legacy per- and polyfluoroalkyl substances in water, sediment, and air of the Bohai Sea and its surrounding rivers. Environ. Pollut. 263, 114391. https://doi.org/10.1016/j.envpol.2020.114391.
Zheng, H., Wang, F., Zhao, Z., Ma, Y., Yang, H., Lu, Z., Cai, M., Cai, M., 2017. Distribution profiles of per- and poly fluoroalkyl substances (PFASs) and their re-regulation by ocean currents in the East and South China Sea. Mar. Pollut. Bull. 125, 481–486. https://doi.org/10.1016/j.marpolbul.2017.08.009.
Zhong, H., Zheng, M., Liang, Y., Wang, Y., Gao, W., Wang, Y., Jiang, G., 2021. Legacy and emerging per- and polyfluoroalkyl substances (PFAS) in sediments from the East China Sea and the Yellow Sea: occurrence, source apportionment and environmental risk assessment. Chemosphere 282, 131042. https://doi.org/10.1016/j.chemosphere.2021.131042.
Zhu, J., Fu, Y., Hu, H., Zhong, Y., Ma, X., Zhu, Y., Zhou, F., Pan, Y., Ma, Y., 2025. Regulation of terrestrial input and ocean processes on the occurrence and transport of traditional and emerging per- and polyfluoroalkyl substances in the inner shelf of the East China Sea. Water Res. 268, 122606. https://doi.org/10.1016/j.watres.2024.122606.

<Supplementary Materials>

Distributions and compositional characteristics of per- and polyfluoroalkyl substances (PFASs) in sediments of the regional seas of South Korea

Sunmi Yang, Jiyun Gwak, Jihyun Cha, Kiho Park, Youngnam Kim, Sea-Yong Kim, Yeonjung Lee, Dong Han Choi, Kongtae Ra, Hyo-Bang Moon, Seongjin Hong *

This PDF file includes:

Number of pages: 26

Number of Supplementary Tables: 13, Tables S1 to S13

Number of Supplementary Figures: 5, Figs. S1 to S5

References

***Corresponding author.**

Department of Earth, Environmental & Space Sciences, Chungnam National University,

99 Daehak-ro, Yuseong-gu, Daejeon 34134, Republic of Korea.

Tel.: +82 42 821 6436; fax: +82 42 822 8173. *E-mail*: hongseongjin@cnu.ac.kr

Supplementary Tables

Table S1. Information on sampling sites, time, location, organic carbon (OC), total nitrogen (TN), and stable isotope ratios ($\delta^{13}C$ and $\delta^{15}N$) in surface sediments (n = 33) of the regional seas of South Korea.

Regional sea	Station	Year	Month	Latitude	Longitude	OC (%)	TN (%)	$\delta^{13}C$ (‰)	$\delta^{15}N$ (‰)	C/N ratio
Yellow Sea	Y1	2024	1	37° 00.07 N	124° 00.37 E	0.34	0.05	–22.54	NA[a]	6.6
	Y2	2024	1	36° 59.57 N	124° 29.52 E	0.12	0.02	–22.04	NA	6.2
	Y3	2024	1	34° 59.54 N	122° 04.17 E	0.47	0.08	–22.17	NA	6.1
	Y4	2024	1	34° 59.58 N	122° 30.03 E	0.90	0.14	–22.18	NA	6.4
	Y5	2024	1	34° 59.58 N	122° 59.57 E	0.90	0.14	–22.13	NA	6.6
	Y6	2024	1	34° 59.53 N	123° 29.54 E	0.97	0.15	–22.06	NA	6.5
	Y7	2024	1	34° 59.56 N	123° 59.55 E	0.57	0.08	–22.22	NA	6.8
	Y8	2024	1	34° 59.59 N	124° 29.59 E	0.61	0.09	–22.14	NA	6.7
	Y9	2024	1	34° 59.52 N	124° 59.59 E	0.16	0.03	–22.15	NA	5.4
	Y10	2024	1	35° 00.02 N	125° 40.45 E	0.79	0.12	–21.65	NA	6.7
East China Sea	EC1	2024	1	32° 10.48 N	123° 59.59 E	0.36	0.06	–20.91	NA	6.3
	EC2	2024	1	32° 12.28 N	124° 30.02 E	0.34	0.06	–20.89	NA	6.1
	EC3	2024	1	32° 10.50 N	124° 59.54 E	0.37	0.06	–21.33	NA	6.2
	EC4	2024	1	32° 11.45 N	125° 30.02 E	0.64	0.11	–21.42	NA	6.0
	EC5	2024	1	32° 11.46 N	125° 59.22 E	0.68	0.11	–21.37	NA	6.0
	EC6	2024	1	32° 11.01 N	126° 30.14 E	0.58	0.09	–21.18	NA	6.2
South Sea	S1	2023	5	33° 51.05 N	127° 38.30 E	0.86	0.12	–21.53	3.56	7.1
	S2	2023	5	33° 47.57 N	127° 02.30 E	1.13	0.17	–21.45	3.12	6.7
	S3	2023	5	34° 23.47 N	128° 24.20 E	1.27	0.20	–21.60	5.92	6.4
	S4	2023	5	34° 41.53 N	128° 52.08 E	1.34	0.20	–21.22	5.11	6.7
	S5	2023	5	34° 57.41 N	129° 20.29 E	0.16	0.04	–21.57	2.37	3.7
East Sea	C1	2023	4	35° 23.03 N	129° 54.37 E	0.21	NA	NA	NA	NA
	C2	2023	4	35° 44.59 N	130° 36.09 E	3.04	NA	NA	NA	NA
	C3	2023	4	36° 07.55 N	130° 55.55 E	3.50	NA	NA	NA	NA
	C4	2023	4	36° 31.17 N	130° 14.15 E	3.19	NA	NA	NA	NA
	C5	2023	4	36° 31.17 N	130° 53.29 E	3.34	NA	NA	NA	NA
	C6	2023	4	36° 31.17 N	131° 32.43 E	3.05	NA	NA	NA	NA
	C7	2023	4	36° 56.22 N	129° 32.17 E	2.34	NA	NA	NA	NA
	C8	2023	4	36° 56.22 N	130° 12.26 E	2.63	NA	NA	NA	NA
	C9	2023	4	36° 56.22 N	130° 52.34 E	2.76	NA	NA	NA	NA
	C10	2023	4	36° 56.22 N	131° 32.43 E	2.90	NA	NA	NA	NA
	C11	2023	4	37° 19.07 N	130° 15.20 E	2.26	NA	NA	NA	NA
	C12	2023	4	37° 19.07 N	131° 32.43 E	2.85	0.40	–21.59	6.20	6.2

[a] NA: not analyzed.

Table S2. Information on target compounds, internal standards, CAS numbers, and standard materials used in this study.

Target compounds	Abbreviation	CAS number	Supplier, purity, and concentration
Perfluoro-n-butanoic acid	PFBA	375-22-4	PFAC-MXH (mixture)
Perfluoro-n-pentanoic acid	PFPeA	2706-90-3	Wellington Laboratories >98%
Perfluoro-n-hexanoic acid	PFHxA	307-24-4	1000-4000 ng/mL ± 5% of the single compounds
Perfluoro-n-heptanoic acid	PFHpA	375-85-9	
Perfluoro-n-octanoic acid	PFOA	335-67-1	
Perfluoro-n-nonanoic aicd	PFNA	375-95-1	
Perfluoro-n-decanoic acid	PFDA	335-76-2	
Perfluoro-n-undecanoic aicd	PFUnDA	2058-94-8	
Perfluoro-n-dodecanoic aicd	PFDoDA	307-55-1	
Perfluoro-n-tridecanoic acid	PFTriDA	72629-94-8	
Perfluoro-n-tetradecanoic aicd	PFTeDA	376-06-7	
Potassium perfluoro-1-butanesulfonate	L-PFBS	29420-49-3	PFAC-MXH (mixture)
Sodium perfluoro-1-pentanesulfonate	L-PFPeS	630402-22-1	Wellington Laboratories >98% 1000-4000 ng/mL ± 5% of the single compounds
Sodium perfluoro-1-hexanesulfonate	L-PFHxS	82382-12-5	L-PFHxS Wellington Laboratories >98 % 50 ± 2.5 µg/mL
Potassium perfluorohexanesulfonate (linear and branched isomers)	br-PFHxS	3871-99-6	PFAC-MXH (mixture) Wellington Laboratories >98% 1000-4000 ng/mL ± 5% of the single compounds
Sodium perfluoro-1-octanesulfonate	L-PFOS	4021-47-0	L-PFOS Wellington Laboratories >98 % 50 ± 2.5 µg/mL
Potassium perfluorooctanesulfonate (linear and branched isomers)	br-PFOS	2795-39-3	PFAC-MXH (mixture) Wellington Laboratories >98%
Sodium perfluoro-1-heptanesulfonate	L-PFHpS	21934-50-9	1000-4000 ng/mL ± 5% of the single compounds
Sodium perfluoro-1-nonanesulfonate	L-PFNS	98789-57-2	
Sodium perfluoro-1-decanesulfonate	L-PFDS	2806-15-7	
N-methylperfluorooctanesulfonamidoacetic acid (linear and branched isomers)	N-MeFOSAA	2355-31-9	PFAC-MXH (mixture) Wellington Laboratories >98%
N-ethylperfluorooctanesulfonamidoacetic acid (linear and branched isomers)	N-EtFOSAA	1336-61-4	1000-4000 ng/mL ± 5% of the single compounds
Sodium 1H, 1H, 2H, 2H-perfluorohexanesulfonate	4:2 FTS	27619-93-8	
Sodium 1H, 1H, 2H, 2H-perfluorooctanesulfonate	6:2 FTS	27619-94-9	

Sodium 1H, 1H, 2H, 2H-perfluorodecanesulfonate	8:2 FTS	27619-96-1	
Sodium dodecafluoro-3H-4, 8-dioxanonanoate	ADONA	958445-44-8	NaDONA Wellington Laboratories >98 % 50 ± 2.5 µg/mL
2,3,3,3-Tetrafluoro-2-(1,1,2,2,3,3,3-heptafluoropropoxy)-propanoic acid	Gen-X	13252-13-6	HFPO-DA (trade name: Gen-X Wellington Laboratories >98 % 50 ± 2.5 µg/mL
Potassium 9-chlorohexadecafluoro-3-oxanonane-1-sulfonate	F53B	73606-19-6	9Cl-PF3ONS Wellington Laboratories >98 % 50 ± 2.5 µg/mL
Perfluoro-n-[1,2-$^{13}C_2$]decanoic acid	MPFDA	960315-50-8	MPFAC-MXA (mixture)
Perfluoro-n-[1,2-$^{13}C_2$]dodecanoic acid	MPFDoDA	960315-52-0	Wellington Laboratories >98%
Perfluoro-n-[1,2-$^{13}C_2$]hexanoic acid	MPFHxA	307-24-4	2000 ng/mL ± 5% of the single compounds
Perfluoro-n-[1,2,3,4,5-$^{13}C_5$]nonanoic acid	MPFNA	960315-49-5	
Perfluoro-n-[1,2,3,4-$^{13}C_4$]octanoic acid	MPFOA	960315-48-4	
Perfluoro-n-[1,2-$^{13}C_2$]undecanoic acid	MPFUdA	960315-51-9	

Table S3. Instrumental conditions for analyzing 28 per- and polyfluoroalkyl substances (PFASs) in sediments using HPLC-MS/MS.

Liquid chromatography	Agilent Infinity 1290 II					
Column	Acquity UPLC BEH Shield RP_{18}, 2.1 x 100 mm, 1.7 um (Waters)					
Column temperature	30 ℃					
Mobile phase	A: Water; B: 80:20 MeOH:ACN (both with 10mM NH_4Ac buffer)					
Gradient mode	Time (min)	0.0	6.0	7.0	7.5	9.0
	A (%)	70	10	10	70	70
	B (%)	30	90	90	30	30
Injection volume	5 μL					
Flow rate	0.3 mL min^{-1}					
Mass spectrometer	Agilent 6470 triple quadrupole mass spectrometer					
Ionization mode	ESI (-) MRM					
Ion spray voltage	2500 V (negative)					
Gas temperature	230 ℃					
Sheath gas temperature	250 ℃					
Nebulizer gas	N_2 (15 psi)					
Sheath gas flow	12 L min^{-1}					

Table S4. Optimized compound-specific parameters in a tandem mass spectrometer for analyzing 28 PFASs and 6 internal standards.

Compounds	Molecular weight	RT (min)	Precursor ion (m/z)	Product ion (m/z)	Fragmentor (volts)	CE (volts)
PFCAs						
PFBA	212.97	2.129	213.0 $[M-H]^-$	168.9	80	5
PFPeA	262.97	3.174	263.0 $[M-H]^-$	218.9	70	5
PFHxA	312.97	4.047	313.0 $[M-H]^-$	118.8	60	25
				268.8	60	5
PFHpA	362.96	4.714	363.0 $[M-H]^-$	168.9	70	15
				318.8	70	5
PFOA	412.96	5.249	413.0 $[M-H]^-$	168.7	70	10
				368.8	70	5
PFNA	462.96	5.684	463.0 $[M-H]^-$	168.6	80	20
				418.9	80	5
PFDA	512.96	6.047	513.0 $[M-H]^-$	218.7	80	15
				468.9	80	5
PFUnDA	562.95	6.357	563.0 $[M-H]^-$	268.9	80	10
				518.8	80	5
PFDoDA	612.95	6.621	613.0 $[M-H]^-$	318.6	90	10
				568.8	90	5
PFTriDA	662.95	6.852	663.0 $[M-H]^-$	219.1	90	20
				618.7	90	10
PFTeDA	712.94	7.043	712.9 $[M-H]^-$	368.9	120	20
				668.9	120	10
PFSAs						
L-PFBS	298.94	3.551	298.9 $[M-H]^-$	80	130	40
				98.9	130	35
L-PFPeS	348.93	4.317	348.9 $[M-H]^-$	79.8	130	40
				98.5	130	35
L-PFHxS	398.93	4.746	398.9 $[M-H]^-$	79.8	140	40
				98.8	140	35
br-PFHxS	398.93	4.899	398.9 $[M-H]^-$	79.8	130	40
				98.7	130	40
L-PFOS	498.93	5	498.9 $[M-H]^-$	79.8	120	40
				98.6	120	40
br-PFOS	498.93	5.766	498.9 $[M-H]^-$	79.9	110	40
L-PFHpS	448.93	5.374	448.9 $[M-H]^-$	79.8	90	40
				98.8	90	40
L-PFNS	548.92	6.106	548.9 $[M-H]^-$	79.8	150	40
				98.8	150	40
L-PFDS	598.92	6.403	598.9 $[M-H]^-$	79.8	150	40
Precursors						
N-MeFOSAA	569.96	6.165	570.0 $[M-H]^-$	419.0	130	15
N-EtFOSAA	583.98	6.324	584.0 $[M-H]^-$	418.8	140	15
4:2 FTS	326.97	3.874	327.0 $[M-H]^-$	80.8	110	20
				306.0	110	20
6:2 FTS	426.96	5.155	427.0 $[M-H]^-$	81.1	120	30
				407.0	120	20
8:2 FTS	526.96	5.994	527.0 $[M-H]^-$	81.1	160	30
				506.8	160	25
Alternatives						
ADONA	376.96	4.799	377.0 $[M-H]^-$	84.8	70	20
				250.8	70	10
Gen-X	328.96	4.311	329.0 $[M-H]^-$	168.6	60	5

				285.0	60	5
F53B	530.89	5.994	530.9 $[M-H]^-$	350.3	130	25
Internal standards						
MPFDA	514.97	6.047	515.0 $[M-H]^-$	468.9	90	5
				514.8	90	5
MPFDoDA	614.96	6.621	615.0 $[M-H]^-$	268.9	100	20
				569.9	100	5
MPFHxA	314.98	4.047	315.0 $[M-H]^-$	269.9	70	5
				314.9	70	5
MPFNA	468.00	5.684	468.0 $[M-H]^-$	222.7	80	10
				422.8	80	5
MPFOA	416.99	5.248	417.0 $[M-H]^-$	171.8	80	20
				371.8	80	5
MPFUdA	564.97	6.357	565.0 $[M-H]^-$	318.7	90	15
				519.8	90	5

Table S5. Linear range, coefficient of determination (R^2), limit of detection (LOD), and limit of quantification (LOQ) of 28 PFASs using LC-MS/MS.

Compounds	Linear range (ng mL^{-1})	R^2	LOD (ng g^{-1} dw)	LOQ (ng g^{-1} dw)
PFBA	0.1–50	0.997	0.07	0.22
PFPeA	0.1–50	0.999	0.03	0.10
PFHxA	0.1–50	0.999	0.01	0.04
PFHpA	0.1–50	0.999	0.01	0.02
PFOA	0.1–50	0.998	0.02	0.06
PFNA	0.1–50	0.999	0.03	0.08
PFDA	0.1–50	0.998	0.02	0.08
PFUnDA	0.1–50	0.998	0.01	0.05
PFDoDA	0.1–50	0.999	0.01	0.02
PFTriDA	0.1–50	0.999	0.02	0.06
PFTeDA	0.1–50	0.999	0.02	0.06
L-PFBS	0.1–50	0.999	0.03	0.09
L-PFPeS	0.1–50	0.999	0.04	0.13
L-PFHxS	0.1–50	0.999	0.07	0.22
br-PFHxS	0.1–50	0.998	0.02	0.05
L-PFOS	0.1–50	0.997	0.08	0.26
br-PFOS	0.1–50	0.999	0.04	0.12
L-PFHpS	0.1–50	0.998	0.04	0.12
L-PFNS	0.1–50	0.998	0.04	0.11
L-PFDS	0.1–50	0.999	0.08	0.26
N-MeFOSAA	0.1–50	0.999	0.05	0.17
N-EtFOSAA	0.1–50	0.998	0.08	0.25
4:2 FTS	0.1–50	0.999	0.16	0.49
6:2 FTS	0.1–50	0.999	0.11	0.34
8:2 FTS	0.1–50	0.994	0.10	0.31
ADONA	0.1–50	0.999	0.02	0.05
Gen-X	0.1–50	0.998	0.02	0.07
F53B	0.1–50	0.998	0.05	0.15

Table S6. Average recovery rates and standard deviation of internal standards obtained in this study.

Compound	Recovery rates (%)	
	Mean	SD [a]
MPFDA	75	9.2
MPFDoA	82	13
MPFNA	68	9.4
MPFOA	74	7.9
MPFUdA	76	9.9
MPFHxA	78	7.1

[a] SD: standard deviation.

Table S7. Concentrations of PFASs in surface and core sediments of the regional seas in South Korea (ng g^{-1} dw).

Sites	Y1	Y2	Y3	Y4	Y5	Y6	Y7	Y8	Y9	Y10	EC1	EC2
PFBA	<LOD	<LOD	<LOD	<LOD	<LOD	<LOD	<LOD	<LOD	<LOD	<LOD	<LOD	<LOD
PFPeA	<LOD	<LOD	<LOD	<LOD	<LOD	<LOD	<LOD	<LOD	<LOD	<LOD	<LOD	<LOD
PFHxA	0.04	<LOD	<LOQ	<LOQ	<LOQ	<LOQ	<LOQ	<LOQ	<LOQ	<LOQ	<LOD	<LOQ
PFHpA	0.04	<LOD	0.03	0.04	0.02	0.03	0.03	0.02	<LOQ	0.03	<LOQ	<LOQ
PFOA	1.2	0.11	0.99	1.5	0.87	1.1	0.26	0.73	0.96	1.1	0.39	0.35
PFNA	0.21	<LOQ	0.19	0.33	0.22	0.41	0.10	0.41	0.25	0.27	0.10	0.10
PFDA	<LOQ	<LOD	<LOQ	0.09	<LOQ	0.12	<LOQ	0.15	<LOQ	<LOQ	<LOQ	<LOQ
PFUnDA	0.12	0.05	0.12	0.21	0.16	0.26	0.17	0.27	0.08	0.14	0.11	0.08
PFDoDA	<LOQ	<LOQ	<LOQ	<LOQ	<LOQ	0.03	0.02	0.03	<LOQ	<LOQ	<LOQ	<LOQ
PFTrIDA	0.06	<LOQ	<LOQ	0.09	0.09	0.14	0.08	0.11	<LOQ	<LOQ	<LOQ	<LOQ
PFTeDA	<LOD	<LOD	<LOD	<LOD	<LOD	<LOD	<LOD	<LOD	<LOD	<LOD	<LOD	<LOD
L-PFBS	<LOD	<LOD	<LOD	<LOD	<LOD	<LOD	<LOD	<LOD	<LOD	<LOD	<LOD	<LOD
L-PFPeS	<LOD	<LOD	<LOD	<LOD	<LOD	<LOD	<LOD	<LOD	<LOD	<LOD	<LOD	<LOD
L-PFHxS	<LOD	<LOD	<LOD	<LOD	<LOD	<LOD	<LOD	<LOD	<LOD	<LOD	<LOD	<LOD
br-PFHxS	<LOD	<LOD	<LOD	<LOD	<LOD	<LOD	<LOD	<LOD	<LOD	<LOD	<LOD	<LOD
L-PFOS	<LOD	<LOD	<LOD	<LOQ	<LOD	<LOQ	<LOD	<LOQ	<LOD	<LOQ	<LOD	<LOD
br-PFOS	<LOQ	<LOD	<LOQ	0.14	<LOQ	0.18	<LOQ	0.17	<LOQ	<LOQ	<LOQ	<LOQ
L-PFHpS	<LOD	<LOD	<LOD	<LOD	<LOD	<LOD	<LOD	<LOD	<LOD	<LOD	<LOD	<LOD
L-PFNS	<LOD	<LOD	<LOD	<LOD	<LOD	<LOD	<LOD	<LOD	<LOD	<LOD	<LOD	<LOD
L-PFDS	<LOD	<LOD	<LOD	<LOD	<LOD	<LOD	<LOD	<LOD	<LOD	<LOD	<LOD	<LOD
N-MeFOSAA	<LOD	<LOD	<LOD	<LOD	<LOD	<LOD	<LOD	<LOD	<LOD	<LOD	<LOD	<LOD
N-EtFOSAA	<LOD	<LOD	<LOD	<LOD	<LOD	<LOD	<LOD	<LOD	<LOD	<LOD	<LOD	<LOD
4:2FTS	<LOD	<LOD	<LOD	<LOD	<LOD	<LOD	<LOD	<LOD	<LOD	<LOD	<LOD	<LOD
6:2FTS	<LOD	<LOD	<LOD	<LOD	<LOD	<LOD	<LOD	<LOD	<LOD	<LOD	<LOD	<LOD
8:2FTS	<LOD	<LOD	<LOD	<LOD	<LOD	<LOD	<LOD	<LOD	<LOD	<LOD	<LOD	<LOD
ADONA	<LOD	<LOD	<LOD	<LOD	<LOD	<LOD	<LOD	<LOD	<LOD	<LOD	<LOD	<LOD
Gen-X	<LOD	<LOD	<LOD	<LOD	<LOD	<LOD	<LOD	<LOD	<LOD	<LOD	<LOD	<LOD
F53B	<LOD	<LOD	<LOD	<LOD	<LOD	<LOD	<LOD	<LOD	<LOD	<LOD	<LOD	<LOD
∑PFASs	1.7	0.17	1.3	2.4	1.4	2.3	0.67	1.9	1.3	1.6	0.59	0.53

Sites	EC3	EC4	EC5	EC6	S1	S2	S3	S4	S5	E1 0–1 cm	E1 1–2 cm	E1 2–3 cm
PFBA	<LOD	<LOD	<LOD	<LOD	<LOD	<LOD	<LOD	<LOD	<LOD	<LOD	<LOD	<LOD
PFPeA	<LOD	<LOD	<LOD	<LOD	<LOD	<LOD	<LOD	<LOD	<LOD	<LOD	<LOD	<LOD
PFHxA	<LOQ	<LOD	<LOQ	<LOD	<LOD	<LOD	<LOD	<LOD	<LOD	<LOD	<LOD	<LOD
PFHpA	<LOQ	<LOQ	<LOQ	<LOQ	<LOD	<LOD	<LOD	<LOD	<LOD	<LOQ	<LOD	<LOD
PFOA	0.32	0.33	0.34	0.24	0.11	0.11	0.14	<LOQ	<LOQ	0.13	0.08	<LOQ
PFNA	0.10	0.13	0.12	0.13	<LOQ	<LOQ	<LOQ	<LOQ	<LOD	<LOQ	<LOQ	<LOQ
PFDA	<LOQ	<LOQ	<LOQ	<LOQ	<LOD	<LOD	<LOD	<LOD	<LOD	<LOQ	<LOQ	<LOQ
PFUnDA	0.07	0.10	0.08	0.07	0.07	0.08	0.10	0.05	<LOQ	0.11	0.12	0.10
PFDoDA	<LOD	<LOQ	<LOQ	<LOQ	<LOQ	<LOQ	<LOQ	<LOQ	<LOD	<LOQ	0.02	0.02
PFTrIDA	<LOQ	<LOQ	<LOQ	<LOQ	<LOQ	0.07	0.08	<LOQ	<LOQ	0.08	0.09	0.08
PFTeDA	<LOD	<LOD	<LOD	<LOD	<LOD	<LOD	<LOD	<LOD	<LOD	<LOD	<LOD	<LOD
L-PFBS	<LOD	<LOD	<LOD	<LOD	<LOD	<LOD	<LOD	<LOD	<LOD	<LOD	<LOD	<LOD
L-PFPeS	<LOD	<LOD	<LOD	<LOD	<LOD	<LOD	<LOD	<LOD	<LOD	<LOD	<LOD	<LOD
L-PFHxS	<LOD	<LOD	<LOD	<LOD	<LOD	<LOD	<LOD	<LOD	<LOD	<LOD	<LOD	<LOD
br-PFHxS	<LOD	<LOD	<LOD	<LOD	<LOD	<LOD	<LOD	<LOD	<LOD	<LOD	<LOD	<LOD
L-PFOS	<LOD	<LOD	<LOD	<LOD	<LOD	<LOD	<LOD	<LOD	<LOD	<LOD	<LOD	<LOD
br-PFOS	<LOQ	<LOQ	<LOQ	<LOD	<LOD	<LOD	<LOD	<LOD	<LOD	<LOD	<LOD	<LOD
L-PFHpS	<LOD	<LOD	<LOD	<LOD	<LOD	<LOD	<LOD	<LOD	<LOD	<LOD	<LOD	<LOD
L-PFNS	<LOD	<LOD	<LOD	<LOD	<LOD	<LOD	<LOD	<LOD	<LOD	<LOD	<LOD	<LOD
L-PFDS	<LOD	<LOD	<LOD	<LOD	<LOD	<LOD	<LOD	<LOD	<LOD	<LOD	<LOD	<LOD
N-MeFOSAA	<LOD	<LOD	<LOD	<LOD	<LOD	<LOD	<LOD	<LOD	<LOD	<LOD	<LOD	<LOD
N-EtFOSAA	<LOD	<LOD	<LOD	<LOD	<LOD	<LOD	<LOD	<LOD	<LOD	<LOD	<LOD	<LOD
4:2FTS	<LOD	<LOD	<LOD	<LOD	<LOD	<LOD	<LOD	<LOD	<LOD	<LOD	<LOD	<LOD
6:2FTS	<LOD	<LOD	<LOD	<LOD	<LOD	<LOD	<LOD	<LOD	<LOD	<LOD	<LOD	<LOD
8:2FTS	<LOD	<LOD	<LOD	<LOD	<LOD	<LOD	<LOD	<LOD	<LOD	<LOD	<LOD	<LOD
ADONA	<LOD	<LOD	<LOD	<LOD	<LOD	<LOD	<LOD	<LOD	<LOD	<LOD	<LOD	<LOD
Gen-X	<LOD	<LOD	<LOD	<LOD	<LOD	<LOD	<LOD	<LOD	<LOD	<LOD	<LOD	<LOD
F53B	<LOD	<LOD	<LOD	<LOD	<LOD	<LOD	<LOD	<LOD	<LOD	<LOD	<LOD	<LOD
∑PFASs	0.49	0.55	0.55	0.43	0.17	0.26	0.32	0.05	N.D	0.31	0.32	0.20

Sites	E1 3–4 cm	E1 4–5 cm	E1 5–6 cm	E1 6–7 cm	E1 7–8 cm	E1 8–9 cm	E1 9–10 cm	E1 10–12 cm	E1 12–14 cm	E1 14–16 cm	E1 16–18 cm	E1 18–20 cm
PFBA	<LOD	<LOD	<LOD	<LOD	<LOD	<LOD	<LOD	<LOD	<LOD	<LOD	<LOD	<LOD
PFPeA	<LOD	<LOD	<LOD	<LOD	<LOD	<LOD	<LOD	<LOD	<LOD	<LOD	<LOD	<LOD
PFHxA	<LOD	<LOD	<LOD	<LOD	<LOD	<LOD	<LOD	<LOD	<LOD	<LOD	<LOD	<LOD
PFHpA	<LOD	<LOD	<LOD	<LOD	<LOD	<LOD	<LOD	<LOD	<LOD	<LOD	<LOD	<LOD
PFOA	<LOQ	<LOD	<LOD	<LOD	<LOD	<LOD	<LOD	<LOD	<LOD	<LOD	<LOD	<LOD
PFNA	<LOD	<LOD	<LOD	<LOD	<LOD	<LOD	<LOD	<LOD	<LOD	<LOD	<LOD	<LOD
PFDA	<LOD	<LOD	<LOD	<LOD	<LOD	<LOD	<LOD	<LOD	<LOD	<LOD	<LOD	<LOD
PFUnDA	0.10	0.07	0.05	<LOQ	<LOQ	<LOD	<LOD	<LOD	<LOD	<LOD	<LOD	<LOD
PFDoDA	<LOQ	<LOQ	<LOQ	<LOD	<LOD	<LOD	<LOD	<LOD	<LOD	<LOD	<LOD	<LOD
PFTrIDA	0.08	0.07	<LOQ	<LOQ	<LOD	<LOD	<LOD	<LOD	<LOD	<LOD	<LOD	<LOD
PFTeDA	<LOD	<LOD	<LOD	<LOD	<LOD	<LOD	<LOD	<LOD	<LOD	<LOD	<LOD	<LOD
L-PFBS	<LOD	<LOD	<LOD	<LOD	<LOD	<LOD	<LOD	<LOD	<LOD	<LOD	<LOD	<LOD
L-PFPeS	<LOD	<LOD	<LOD	<LOD	<LOD	<LOD	<LOD	<LOD	<LOD	<LOD	<LOD	<LOD
L-PFHxS	<LOD	<LOD	<LOD	<LOD	<LOD	<LOD	<LOD	<LOD	<LOD	<LOD	<LOD	<LOD
br-PFHxS	<LOD	<LOD	<LOD	<LOD	<LOD	<LOD	<LOD	<LOD	<LOD	<LOD	<LOD	<LOD
L-PFOS	<LOD	<LOD	<LOD	<LOD	<LOD	<LOD	<LOD	<LOD	<LOD	<LOD	<LOD	<LOD
br-PFOS	<LOD	<LOD	<LOD	<LOD	<LOD	<LOD	<LOD	<LOD	<LOD	<LOD	<LOD	<LOD
L-PFHpS	<LOD	<LOD	<LOD	<LOD	<LOD	<LOD	<LOD	<LOD	<LOD	<LOD	<LOD	<LOD
L-PFNS	<LOD	<LOD	<LOD	<LOD	<LOD	<LOD	<LOD	<LOD	<LOD	<LOD	<LOD	<LOD
L-PFDS	<LOD	<LOD	<LOD	<LOD	<LOD	<LOD	<LOD	<LOD	<LOD	<LOD	<LOD	<LOD
N-MeFOSAA	<LOD	<LOD	<LOD	<LOD	<LOD	<LOD	<LOD	<LOD	<LOD	<LOD	<LOD	<LOD
N-EtFOSAA	<LOD	<LOD	<LOD	<LOD	<LOD	<LOD	<LOD	<LOD	<LOD	<LOD	<LOD	<LOD
4:2FTS	<LOD	<LOD	<LOD	<LOD	<LOD	<LOD	<LOD	<LOD	<LOD	<LOD	<LOD	<LOD
6:2FTS	<LOD	<LOD	<LOD	<LOD	<LOD	<LOD	<LOD	<LOD	<LOD	<LOD	<LOD	<LOD
8:2FTS	<LOD	<LOD	<LOD	<LOD	<LOD	<LOD	<LOD	<LOD	<LOD	<LOD	<LOD	<LOD
ADONA	<LOD	<LOD	<LOD	<LOD	<LOD	<LOD	<LOD	<LOD	<LOD	<LOD	<LOD	<LOD
Gen-X	<LOD	<LOD	<LOD	<LOD	<LOD	<LOD	<LOD	<LOD	<LOD	<LOD	<LOD	<LOD
F53B	<LOD	<LOD	<LOD	<LOD	<LOD	<LOD	<LOD	<LOD	<LOD	<LOD	<LOD	<LOD
∑PFASs	0.18	0.15	0.05	0	0	0	0	0	0	0	0	0

Sites	E1 20–22 cm	E1 22–24 cm	E1 24–26 cm	E1 26–28 cm	E1 28–30 cm	E2 0–1 cm	E3 0–1 cm	E3 1–2 cm	E3 2–3 cm	E3 3–4 cm	E3 4–5 cm	E3 5–6 cm
PFBA	<LOD	<LOD	<LOD	<LOD	<LOD	<LOD	<LOD	<LOD	<LOD	<LOD	<LOD	<LOD
PFPeA	<LOD	<LOD	<LOD	<LOD	<LOD	<LOD	<LOD	<LOD	<LOD	<LOD	<LOD	<LOD
PFHxA	<LOD	<LOD	<LOD	<LOD	<LOD	<LOQ	0.05	0.04	<LOQ	<LOQ	<LOQ	<LOQ
PFHpA	<LOD	<LOD	<LOD	<LOD	<LOD	0.04	0.11	0.05	0.04	0.03	0.03	0.03
PFOA	<LOD	<LOD	<LOD	<LOD	<LOD	0.21	0.38	0.14	0.09	0.09	0.09	0.09
PFNA	<LOD	<LOD	<LOD	<LOD	<LOD	0.11	0.32	0.13	0.10	0.10	0.10	0.11
PFDA	<LOD	<LOD	<LOD	<LOD	<LOD	0.43	1.6	0.76	0.43	0.36	0.33	0.32
PFUnDA	<LOQ	<LOQ	<LOD	<LOD	<LOD	2.4	10	7.3	4.4	3.3	3.0	2.4
PFDoDA	<LOD	<LOD	<LOD	<LOD	<LOD	0.25	0.82	0.94	0.60	0.48	0.50	0.40
PFTrIDA	<LOD	<LOD	<LOD	<LOD	<LOD	0.66	1.7	2.0	1.3	0.98	0.94	0.78
PFTeDA	<LOD	<LOD	<LOD	<LOD	<LOD	<LOQ	0.13	0.16	0.10	0.07	0.07	0.07
L-PFBS	<LOD	<LOD	<LOD	<LOD	<LOD	<LOD	<LOD	<LOD	<LOD	<LOQ	<LOQ	<LOQ
L-PFPeS	<LOD	<LOD	<LOD	<LOD	<LOD	<LOD	<LOD	<LOD	<LOD	<LOD	<LOD	<LOD
L-PFHxS	<LOD	<LOD	<LOD	<LOD	<LOD	<LOD	<LOD	<LOD	<LOD	<LOD	<LOD	<LOD
br-PFHxS	<LOD	<LOD	<LOD	<LOD	<LOD	<LOD	<LOD	<LOD	<LOD	<LOD	<LOD	<LOD
L-PFOS	<LOD	<LOD	<LOD	<LOD	<LOD	<LOQ	<LOQ	<LOQ	<LOQ	<LOQ	<LOQ	<LOQ
br-PFOS	<LOD	<LOD	<LOD	<LOD	<LOD	0.14	0.15	<LOQ	<LOQ	<LOQ	<LOQ	<LOQ
L-PFHpS	<LOD	<LOD	<LOD	<LOD	<LOD	<LOD	<LOD	<LOD	<LOD	<LOD	<LOD	<LOD
L-PFNS	<LOD	<LOD	<LOD	<LOD	<LOD	<LOD	<LOD	<LOD	<LOD	<LOD	<LOD	<LOD
L-PFDS	<LOD	<LOD	<LOD	<LOD	<LOD	<LOD	<LOD	<LOD	<LOD	<LOD	<LOQ	<LOQ
N-MeFOSAA	<LOD	<LOD	<LOD	<LOD	<LOD	<LOD	<LOQ	<LOQ	<LOQ	<LOQ	<LOQ	<LOQ
N-EtFOSAA	<LOD	<LOD	<LOD	<LOD	<LOD	<LOD	<LOD	<LOD	<LOD	<LOD	<LOD	<LOD
4:2FTS	<LOD	<LOD	<LOD	<LOD	<LOD	<LOD	<LOD	<LOD	<LOD	<LOD	<LOD	<LOD
6:2FTS	<LOD	<LOD	<LOD	<LOD	<LOD	<LOD	<LOQ	<LOD	<LOD	<LOD	<LOD	<LOD
8:2FTS	<LOD	<LOD	<LOD	<LOD	<LOD	<LOD	<LOQ	0.48	<LOQ	<LOQ	<LOQ	<LOQ
ADONA	<LOD	<LOD	<LOD	<LOD	<LOD	<LOD	<LOD	<LOD	<LOD	<LOD	<LOD	<LOD
Gen-X	<LOD	<LOD	<LOD	<LOD	<LOD	<LOD	<LOD	<LOD	<LOD	<LOD	<LOD	<LOD
F53B	<LOD	<LOD	<LOD	<LOD	<LOD	<LOD	<LOD	<LOD	<LOD	<LOD	<LOD	<LOD
∑PFASs	0	0	0	0	0	4.2	16	12	7.1	5.4	5.1	4.2

Sites	E3 6–7 cm	E3 7–8 cm	E3 8–9 cm	E3 9–10 cm	E3 10–12 cm	E3 12–14 cm	E3 14–16 cm	E3 16–18 cm	E3 18–20 cm	E3 20–22 cm	E3 22–24 cm	E3 24–26 cm
PFBA	<LOD	<LOD	<LOD	<LOD	<LOD	<LOD	<LOD	<LOD	<LOD	<LOD	<LOD	<LOD
PFPeA	<LOD	<LOD	<LOD	<LOD	<LOD	<LOD	<LOD	<LOD	<LOD	<LOD	<LOD	<LOD
PFHxA	0.05	0.07	<LOQ	<LOQ	<LOD	<LOD	<LOD	<LOD	<LOD	<LOD	<LOD	<LOD
PFHpA	0.05	0.06	0.04	0.02	<LOQ	<LOD	<LOD	<LOD	<LOD	<LOD	<LOD	<LOD
PFOA	0.15	0.21	0.14	0.09	<LOQ	<LOD	<LOD	<LOD	<LOD	<LOD	<LOD	<LOD
PFNA	0.14	0.22	0.12	0.08	<LOQ	<LOD	<LOD	<LOD	<LOD	<LOD	<LOD	<LOD
PFDA	0.43	0.51	0.36	0.33	0.19	<LOQ	<LOD	<LOD	<LOQ	<LOD	<LOD	<LOD
PFUnDA	2.5	2.3	1.8	2.3	1.7	0.34	0.11	0.08	0.11	0.05	<LOQ	<LOQ
PFDoDA	0.37	0.34	0.27	0.24	0.13	<LOQ	<LOD	<LOD	<LOQ	<LOD	<LOD	<LOD
PFTrIDA	0.65	0.66	0.50	0.35	0.19	<LOQ	<LOD	<LOD	<LOD	<LOD	<LOD	<LOD
PFTeDA	0.08	0.06	<LOQ	<LOQ	<LOD	<LOD	<LOD	<LOD	<LOD	<LOD	<LOD	<LOD
L-PFBS	<LOQ	<LOQ	<LOD	<LOD	<LOD	<LOD	<LOD	<LOD	<LOD	<LOD	<LOD	<LOD
L-PFPeS	<LOD	<LOD	<LOD	<LOD	<LOD	<LOD	<LOD	<LOD	<LOD	<LOD	<LOD	<LOD
L-PFHxS	<LOD	<LOD	<LOD	<LOD	<LOD	<LOD	<LOD	<LOD	<LOD	<LOD	<LOD	<LOD
br-PFHxS	<LOD	<LOD	<LOD	<LOD	<LOD	<LOD	<LOD	<LOD	<LOD	<LOD	<LOD	<LOD
L-PFOS	0.32	<LOQ	<LOQ	<LOD	<LOD	<LOD	<LOD	<LOD	<LOD	<LOD	<LOD	<LOD
br-PFOS	<LOQ	0.13	<LOQ	<LOD	<LOD	<LOD	<LOD	<LOD	<LOD	<LOD	<LOD	<LOD
L-PFHpS	<LOQ	<LOD	<LOD	<LOD	<LOD	<LOD	<LOD	<LOD	<LOD	<LOD	<LOD	<LOD
L-PFNS	<LOQ	<LOQ	<LOD	<LOD	<LOD	<LOD	<LOD	<LOD	<LOD	<LOD	<LOD	<LOD
L-PFDS	<LOQ	<LOQ	<LOD	<LOD	<LOD	<LOD	<LOD	<LOD	<LOD	<LOD	<LOD	<LOD
N-MeFOSAA	<LOQ	<LOQ	<LOQ	<LOQ	<LOQ	<LOD	<LOD	<LOD	<LOD	<LOD	<LOD	<LOD
N-EtFOSAA	<LOD	<LOD	<LOD	<LOD	<LOD	<LOD	<LOD	<LOD	<LOD	<LOD	<LOD	<LOD
4:2FTS	<LOD	<LOD	<LOD	<LOD	<LOD	<LOD	<LOD	<LOD	<LOD	<LOD	<LOD	<LOD
6:2FTS	<LOD	<LOD	<LOD	<LOD	<LOD	<LOD	<LOD	<LOD	<LOD	<LOD	<LOD	<LOD
8:2FTS	0.34	0.34	<LOQ	<LOQ	<LOD	<LOD	<LOD	<LOD	<LOD	<LOD	<LOD	<LOD
ADONA	<LOD	<LOD	<LOD	<LOD	<LOD	<LOD	<LOD	<LOD	<LOD	<LOD	<LOD	<LOD
Gen-X	<LOD	<LOD	<LOD	<LOD	<LOD	<LOD	<LOD	<LOD	<LOD	<LOD	<LOD	<LOD
F53B	<LOD	<LOD	<LOD	<LOD	<LOD	<LOD	<LOD	<LOD	<LOD	<LOD	<LOD	<LOD
∑PFASs	5.1	4.9	3.2	3.4	2.2	0.34	0.11	0.08	0.11	0.05	0	0

Sites	E3 26–28 cm	E3 28–30 cm	E5 0–1 cm	E6 0–1 cm	E7 0–1 cm	E8 0–1 cm	E9 0–1 cm	E10 0–1 cm	E11 0–1 cm	E11 1–2 cm	E11 2–3 cm	E11 3–4 cm
PFBA	<LOD	<LOD	<LOD	<LOD	<LOD	<LOD	<LOD	<LOD	<LOD	<LOD	<LOD	<LOD
PFPeA	<LOD	<LOD	<LOD	<LOD	<LOD	<LOD	<LOQ	<LOQ	<LOD	<LOD	<LOD	<LOD
PFHxA	<LOD	<LOD	0.04	0.07	0.08	<LOQ	0.07	0.10	0.04	<LOD	<LOD	<LOD
PFHpA	<LOD	<LOD	0.09	0.13	0.20	<LOQ	0.18	0.21	0.12	<LOQ	<LOQ	<LOD
PFOA	<LOD	<LOD	0.34	0.41	0.62	0.31	0.52	0.59	0.35	0.09	<LOQ	<LOD
PFNA	<LOD	<LOD	0.22	0.48	0.45	0.35	0.23	0.23	0.16	<LOQ	<LOD	<LOD
PFDA	<LOD	<LOD	0.35	1.10	0.48	0.15	0.29	0.31	0.19	0.107	<LOQ	<LOD
PFUnDA	<LOQ	0.06	1.5	3.2	1.4	0.40	1.3	1.3	0.73	0.39	0.16	<LOQ
PFDoDA	<LOD	<LOD	0.23	0.37	0.20	0.04	0.22	0.23	0.13	0.09	0.04	<LOQ
PFTrIDA	<LOD	<LOD	0.61	0.87	0.59	0.13	0.60	0.63	0.42	0.29	0.11	<LOQ
PFTeDA	<LOD	<LOD	0.08	0.09	0.08	<LOD	0.08	0.08	<LOQ	<LOQ	<LOD	<LOD
L-PFBS	<LOD	<LOD	<LOD	<LOD	<LOD	<LOD	<LOD	<LOD	<LOD	<LOD	<LOD	<LOD
L-PFPeS	<LOD	<LOD	<LOD	<LOD	<LOD	<LOD	<LOD	<LOD	<LOD	<LOD	<LOD	<LOD
L-PFHxS	<LOD	<LOD	<LOD	<LOD	<LOD	<LOD	<LOD	<LOD	<LOD	<LOD	<LOD	<LOD
br-PFHxS	<LOD	<LOD	<LOD	<LOD	<LOD	<LOD	<LOD	<LOD	<LOD	<LOD	<LOD	<LOD
L-PFOS	<LOD	<LOD	<LOQ	<LOQ	<LOD	<LOD	<LOD	<LOD	<LOD	<LOD	<LOD	<LOD
br-PFOS	<LOD	<LOD	0.14	<LOQ	0.16	<LOQ	0.17	0.19	<LOQ	<LOD	<LOD	<LOD
L-PFHpS	<LOD	<LOD	<LOD	<LOD	<LOD	<LOD	<LOD	<LOD	<LOD	<LOD	<LOD	<LOD
L-PFNS	<LOD	<LOD	<LOD	<LOD	<LOD	<LOD	<LOD	<LOD	<LOD	<LOD	<LOD	<LOD
L-PFDS	<LOD	<LOD	<LOD	<LOD	<LOD	<LOD	<LOD	<LOD	<LOD	<LOD	<LOD	<LOD
N-MeFOSAA	<LOD	<LOD	<LOD	<LOD	<LOD	<LOD	<LOD	<LOD	<LOD	<LOD	<LOD	<LOD
N-EtFOSAA	<LOD	<LOD	<LOD	<LOD	<LOD	<LOD	<LOD	<LOD	<LOD	<LOD	<LOD	<LOD
4:2FTS	<LOD	<LOD	<LOD	<LOD	<LOD	<LOD	<LOD	<LOD	<LOD	<LOD	<LOD	<LOD
6:2FTS	<LOD	<LOD	<LOD	<LOD	<LOD	<LOD	<LOD	<LOD	<LOD	<LOD	<LOD	<LOD
8:2FTS	<LOD	<LOD	<LOD	<LOD	<LOD	<LOD	<LOD	<LOD	<LOD	<LOD	<LOD	<LOD
ADONA	<LOD	<LOD	<LOD	<LOD	<LOD	<LOD	<LOD	<LOD	<LOD	<LOD	<LOD	<LOD
Gen-X	<LOD	<LOD	<LOD	<LOD	<LOD	<LOD	<LOD	<LOD	<LOD	<LOD	<LOD	<LOD
F53B	<LOD	<LOD	<LOD	<LOD	<LOD	<LOD	<LOD	<LOD	<LOD	<LOD	<LOD	<LOD
∑PFASs	0	0.06	3.7	6.7	4.3	1.4	3.7	3.9	2.2	0.97	0.31	0

Sites	E11 4–5 cm	E11 5–6 cm	E11 6–7 cm	E11 7–8 cm	E11 8–9 cm	E11 9–10 cm	E11 10–12 cm	E11 12–14 cm	E11 14–16 cm	E11 16–18 cm	E11 18–20 cm	E11 20–22 cm
PFBA	<LOD	<LOD	<LOD	<LOD	<LOD	<LOD	<LOD	<LOD	<LOD	<LOD	<LOD	<LOD
PFPeA	<LOD	<LOD	<LOD	<LOD	<LOD	<LOD	<LOD	<LOD	<LOD	<LOD	<LOD	<LOD
PFHxA	<LOD	<LOD	<LOD	<LOD	<LOD	<LOD	<LOD	<LOD	<LOD	<LOD	<LOD	<LOD
PFHpA	<LOD	<LOD	<LOD	<LOD	<LOD	<LOD	<LOD	<LOD	<LOD	<LOD	<LOD	<LOD
PFOA	<LOD	<LOD	<LOD	<LOD	<LOD	<LOD	<LOD	<LOD	<LOD	<LOD	<LOD	<LOD
PFNA	<LOD	<LOD	<LOD	<LOD	<LOD	<LOD	<LOD	<LOD	<LOD	<LOD	<LOD	<LOD
PFDA	<LOD	<LOD	<LOD	<LOD	<LOD	<LOD	<LOD	<LOD	<LOD	<LOD	<LOD	<LOD
PFUnDA	<LOD	<LOD	<LOD	<LOD	<LOD	<LOD	<LOD	<LOD	<LOD	<LOD	<LOD	<LOD
PFDoDA	<LOD	<LOD	<LOD	<LOD	<LOD	<LOD	<LOD	<LOD	<LOD	<LOD	<LOD	<LOD
PFTrIDA	<LOD	<LOD	<LOD	<LOD	<LOD	<LOD	<LOD	<LOD	<LOD	<LOD	<LOD	<LOD
PFTeDA	<LOD	<LOD	<LOD	<LOD	<LOD	<LOD	<LOD	<LOD	<LOD	<LOD	<LOD	<LOD
L-PFBS	<LOD	<LOD	<LOD	<LOD	<LOD	<LOD	<LOD	<LOD	<LOD	<LOD	<LOD	<LOD
L-PFPeS	<LOD	<LOD	<LOD	<LOD	<LOD	<LOD	<LOD	<LOD	<LOD	<LOD	<LOD	<LOD
L-PFHxS	<LOD	<LOD	<LOD	<LOD	<LOD	<LOD	<LOD	<LOD	<LOD	<LOD	<LOD	<LOD
br-PFHxS	<LOD	<LOD	<LOD	<LOD	<LOD	<LOD	<LOD	<LOD	<LOD	<LOD	<LOD	<LOD
L-PFOS	<LOD	<LOD	<LOD	<LOD	<LOD	<LOD	<LOD	<LOD	<LOD	<LOD	<LOD	<LOD
br-PFOS	<LOD	<LOD	<LOD	<LOD	<LOD	<LOD	<LOD	<LOD	<LOD	<LOD	<LOD	<LOD
L-PFHpS	<LOD	<LOD	<LOD	<LOD	<LOD	<LOD	<LOD	<LOD	<LOD	<LOD	<LOD	<LOD
L-PFNS	<LOD	<LOD	<LOD	<LOD	<LOD	<LOD	<LOD	<LOD	<LOD	<LOD	<LOD	<LOD
L-PFDS	<LOD	<LOD	<LOD	<LOD	<LOD	<LOD	<LOD	<LOD	<LOD	<LOD	<LOD	<LOD
N-MeFOSAA	<LOD	<LOD	<LOD	<LOD	<LOD	<LOD	<LOD	<LOD	<LOD	<LOD	<LOD	<LOD
N-EtFOSAA	<LOD	<LOD	<LOD	<LOD	<LOD	<LOD	<LOD	<LOD	<LOD	<LOD	<LOD	<LOD
4:2FTS	<LOD	<LOD	<LOD	<LOD	<LOD	<LOD	<LOD	<LOD	<LOD	<LOD	<LOD	<LOD
6:2FTS	<LOD	<LOD	<LOD	<LOD	<LOD	<LOD	<LOD	<LOD	<LOD	<LOD	<LOD	<LOD
8:2FTS	<LOD	<LOD	<LOD	<LOD	<LOD	<LOD	<LOD	<LOD	<LOD	<LOD	<LOD	<LOD
ADONA	<LOD	<LOD	<LOD	<LOD	<LOD	<LOD	<LOD	<LOD	<LOD	<LOD	<LOD	<LOD
Gen-X	<LOD	<LOD	<LOD	<LOD	<LOD	<LOD	<LOD	<LOD	<LOD	<LOD	<LOD	<LOD
F53B	<LOD	<LOD	<LOD	<LOD	<LOD	<LOD	<LOD	<LOD	<LOD	<LOD	<LOD	<LOD
∑PFASs	0	0	0	0	0	0	0	0	0	0	0	0

Sites	E11 22–24 cm	E11 24–26 cm	E11 26–28 cm	E11 28–30 cm	E13 0–1 cm	E15 0–1 cm
PFBA	<LOD	<LOD	<LOD	<LOD	<LOD	<LOD
PFPeA	<LOD	<LOD	<LOD	<LOD	<LOD	<LOD
PFHxA	<LOD	<LOD	<LOD	<LOD	<LOQ	0.04
PFHpA	<LOD	<LOD	<LOD	<LOD	0.10	0.08
PFOA	<LOD	<LOD	<LOD	<LOD	0.35	0.23
PFNA	<LOD	<LOD	<LOD	<LOD	0.13	0.10
PFDA	<LOD	<LOD	<LOD	<LOD	0.19	0.12
PFUnDA	<LOD	<LOD	<LOD	<LOD	1.0	1.0
PFDoDA	<LOD	<LOD	<LOD	<LOD	0.15	0.18
PFTrIDA	<LOD	<LOD	<LOD	<LOD	0.44	0.39
PFTeDA	<LOD	<LOD	<LOD	<LOD	<LOQ	<LOQ
L-PFBS	<LOD	<LOD	<LOD	<LOD	<LOD	<LOD
L-PFPeS	<LOD	<LOD	<LOD	<LOD	<LOD	<LOD
L-PFHxS	<LOD	<LOD	<LOD	<LOD	<LOD	<LOD
br-PFHxS	<LOD	<LOD	<LOD	<LOD	<LOD	<LOD
L-PFOS	<LOD	<LOD	<LOD	<LOD	<LOD	<LOD
br-PFOS	<LOD	<LOD	<LOD	<LOD	0.16	<LOQ
L-PFHpS	<LOD	<LOD	<LOD	<LOD	<LOD	<LOD
L-PFNS	<LOD	<LOD	<LOD	<LOD	<LOD	<LOD
L-PFDS	<LOD	<LOD	<LOD	<LOD	<LOD	<LOD
N-MeFOSAA	<LOD	<LOD	<LOD	<LOD	<LOD	<LOD
N-EtFOSAA	<LOD	<LOD	<LOD	<LOD	<LOD	<LOD
4:2FTS	<LOD	<LOD	<LOD	<LOD	<LOD	<LOD
6:2FTS	<LOD	<LOD	<LOD	<LOD	<LOD	<LOD
8:2FTS	<LOD	<LOD	<LOD	<LOD	<LOD	<LOD
ADONA	<LOD	<LOD	<LOD	<LOD	<LOD	<LOD
Gen-X	<LOD	<LOD	<LOD	<LOD	<LOD	<LOD
F53B	<LOD	<LOD	<LOD	<LOD	<LOD	<LOD
∑PFASs	0	0	0	0	2.6	2.2

Table S8. Results of one-way ANOVA and Tukey's HSD post hoc tests for log-transformed PFAS concentrations in surface sediments from the four regional seas (YS, ECS, SS, and ES). Only statistically significant pairwise differences ($p < 0.05$) are shown.

Compound	ANOVA p-value	Significant Comparison	Tukey HSD p-value
PFHxA	< 0.05	YS – ES	< 0.05
	< 0.01	YS – SS	< 0.01
PFOA	< 0.01	ES – ECS	< 0.01
		SS – ECS	< 0.01
		YS – ES	< 0.01
		YS – SS	
PFNA	< 0.01	ES – ECS	< 0.01
		SS – ECS	< 0.01
		YS – ES	< 0.01
		YS – SS	
PFUnDA	< 0.01	ES – ECS	< 0.01
		SS – ES	< 0.01
		YS – SS	< 0.01
PFDoDA	< 0.01	ES – ECS	< 0.05
		SS – ES	< 0.01
		YS – ES	< 0.05
PFTrIDA	< 0.01	ES – ECS	< 0.01
		SS – ES	< 0.01
PFTeDA	< 0.01	ES – ECS	< 0.05
		YS – ES	< 0.01
br.PFOSK	< 0.01	ES – ECS	< 0.05
		YS – ES	< 0.01

Table S9. OC, TN, and stable isotope ratios ($\delta^{13}C$ and $\delta^{15}N$) in core sediments of the East Sea.

Station	Depth (cm)	OC (%)	TN (%)	$\delta^{13}C$ (‰)	$\delta^{15}N$ (‰)
C1	0–1	0.21	NA[a]	NA	NA
	1–2	0.30	0.04	–21.42	5.05
	2–3	0.37	0.05	–21.40	4.74
	3–4	0.61	0.08	–21.16	4.72
	5–6	0.49	0.07	–20.96	2.77
	6–7	0.55	0.07	–20.87	5.08
	7–8	0.58	0.08	–20.76	6.70
	8–9	0.79	0.11	–20.52	4.15
	9–10	0.46	0.06	–20.60	5.25
	12–14	0.36	0.05	–20.85	2.07
	14–16	0.45	0.06	–20.83	3.73
	16–18	0.35	0.05	–20.89	3.83
	20–22	0.50	0.07	–20.71	1.85
	22–24	0.26	0.04	–20.55	4.07
	24–26	0.56	0.08	–20.60	4.11
	26–28	0.55	0.08	–20.68	5.38
	28–30	0.38	0.05	–20.75	3.91
C3	0–1	3.5	NA	NA	NA
	1–2	3.66	0.51	–22.45	4.64
	2–3	3.67	0.51	–22.52	4.95
	3–4	3.62	0.49	–22.43	5.25
	5–6	3.65	0.47	–22.50	5.12
	6–7	4.38	0.54	–22.98	5.00
	7–8	4.23	0.63	–22.81	3.91
	8–9	3.28	0.45	–22.35	5.44
	9–10	2.72	0.41	–21.70	5.10
	12–14	2.39	0.38	–21.21	5.55
	14–16	2.36	0.37	–21.09	5.30
	16–18	2.42	0.37	–21.00	5.90
	20–22	2.36	0.41	–21.08	4.43
	22–24	2.30	0.35	–20.97	6.05
	24–26	2.27	0.33	–20.99	5.59
	26–28	2.26	0.36	–21.04	5.32
	28–30	2.38	0.36	–21.10	5.95
C10	0–1	2.9	NA	NA	NA
	1–2	2.92	0.44	–21.50	5.36
	2–3	2.46	0.37	–21.51	5.40
	3–4	2.10	0.34	–21.28	6.15
	5–6	1.98	0.33	–21.21	6.18
	6–7	1.91	0.29	–21.21	6.09
	7–8	1.89	0.28	–21.18	5.67
	8–9	1.94	0.30	–21.19	6.01
	9–10	1.94	0.31	–21.24	5.66
	12–14	1.79	0.32	–21.35	4.78
	14–16	1.67	0.34	–21.44	3.49
	16–18	1.68	0.27	–21.45	5.91
	20–22	1.91	0.32	–21.42	6.30
	22–24	1.87	0.31	–21.39	5.96
	24–26	2.00	0.33	–21.39	5.85
	26–28	2.04	0.33	–21.36	5.90
	28–30	2.03	0.33	–21.33	5.64

[a] NA: not analyzed.

Table S10. Principal components (PC1 and PC2) derived from PCA using PFAS compositions in surface sediments of the regional seas of South Korea.

Sites	PC1	PC2
Y1	2.3	1.4
Y2	0.46	-3.2
Y3	2.4	1.6
Y4	2.2	1.7
Y5	2.1	1.6
Y6	1.9	1.3
Y7	0.09	-0.29
Y8	1.7	0.78
Y9	2.9	1.7
Y10	2.6	1.8
EC1	1.8	0.09
EC2	1.8	-0.20
EC3	1.8	-0.45
EC4	1.9	-0.10
EC5	2.0	-0.14
EC6	1.9	-0.85
S1	0.38	-3.1
S2	-0.17	-2.4
S3	-0.17	-1.8
S5	-0.06	-5.9
C1	-0.24	-1.8
C2	-3.3	1.7
C3	-3.2	2.1
C4	-3.0	0.69
C5	-3.3	0.94
C6	-2.3	0.12
C7	0.45	0.96
C8	-2.8	0.05
C9	-2.8	-0.32
C10	-3.1	0.28
C11	-2.8	0.84
C12	-3.3	0.98

Table S11. Factor loadings of individual PFAS compounds on two principal components (PC1 and PC2), derived from a PCA based on PFAS compositions in surface sediments from the regional seas of South Korea.

Sites	PC1	PC2
PFHxA	0.057	-0.545
PFHpA	-0.247	-0.189
PFOA	0.409	0.158
PFNA	0.357	0.009
PFDA	-0.299	-0.242
PFUnDA	-0.409	0.157
PFDoDA	-0.432	-0.005
PFTriDA	-0.412	-0.075
PFTeDA	0.106	-0.536
br-PFOS	0.132	-0.515

Table S12. Concentrations of PFASs in water and sediments and water-sediment partition coefficients in this study and previous studies.

Location	Sampling Year	Salinity	Range [a]		Log K_d value [b]				References
			Water (ng L^{-1})	Sediment (ng g^{-1} dw)	C_6 (PFHxA)	C_7 (PFHpA)	C_8 (PFOA)	C_9 (PFNA)	
Lakes and Rivers									
Poyang Lake, China	2019	–	23–3000 (45)	0.26–2.9 (2.1)	0.76±0.41	0.86±0.58	0.70±0.48	1.4±0.28	Tang et al., 2022
Taihu Lake, China	2010	–	10–120 (57)	1.1–8.2 (2.4)	0.86±0.34 (0.07–1.5)	1.4±0.43 (0.91–2.4)	0.65±0.30 (0.45–2.4)	1.9±0.44 (1.1–2.0)	Guo et al., 2015
Dianchi Lake, China	2010	–	36–140	0.21–2.5	1.3±0.37	1.2±0.15	1.3±0.40	1.2±0.21	Zhang et al., 2012
Daling River and its estuary, China	2023	–	200–890 (460)	0.64–240 (120)	–	–	3.3±0.41 (2.2–3.7)	–	Wang et al., 2024
Llobregat River, Spain	2010	–	21–3100 (300)	8.4–38 (8.2)	–	–	2.0 (1.3–2.9)	–	Campo et al., 2015
Coastal area									
Korean coasts, South Korea	2018	–	0.39–23 (4.5)	0.045–1.1 (0.33)	1.7±1.5 (0.4-1.9)	–	2.0±2.2 (0.8–3.0)	–	Lee et al., 2020
South Bohai coastal rivers, China	2011	–	2.2–5100 (320)	0.29–96 (5.4)	0.59±0.33	0.45±0.35	0.63±0.51	1.0±0.49	Zhu et al., 2014
Laizhou Bay, China	2022	27	37–220 (120)	0.99–7.2 (3.0)	0.55±0.35	1.2±0.36	1.3±0.40	2.0±0.41	Liu et al., 2024
South China Sea coastal region, China	2017, 2018	28	0.13–1.0 (0.55)	0.007–0.08 (0.03)	0.149	–	0.071	1.1	Wang et al., 2019
Regional sea									
Beibu Gulf, South China Sea	2019	31	0.93–2.6 (2.0)	0.19–0.66 (0.39)	–	–	2.2±0.22 (1.8–2.8)	2.6±0.24 (2.2–3.1)	Xiao et al., 2021
Bohai Sea, China	2017	25	6.0–940 (76)	0.7–4.1 (1.8)	3.6±0.3	3.7±0.35	2.8±0.57	3.6±0.20	Zhao et al., 2020
South China Sea	2020	30	7.6–16 (13)	0.83–8.9 (3.8)	4.0±11 (N.D–39)	3.9±4.8 (N.D–13)	1.3±2.5 (N.D–8.0)	0.49±1.6 (N.D–5.9)	Diao et al., 2023
Yellow Sea	2024	32	0.19–17 (10)	0.17–2.4 (1.5)	0.18±0.53 (N.D–1.8)	1.5±0.8 (N.D–2.1)	2.0±0.3 (1.3–2.5)	2.3±1.5 (N.D–3.7)	Yang et al., 2025; This study
East China Sea	2024	33	0.26–17 (6.1)	0.43–0.59 (0.52)	–	–	2.1±0.6 (1.5–2.9)	1.2±1.4 (N.D–2.9)	Yang et al., 2025; This study
South Sea	2023	34	0.08–3.4 (1.1)	N.D–0.32 (0.16)	–	–	1.3±1.1 (N.D–2.4)	–	Yang et al., 2025; This study
East Sea	2023	35	N.D–1.4 (0.66)	0.31–16 (4.2)	1.8±1.3 (N.D–2.9)	3.0±1.4 (N.D–3.9)	2.7±0.2 (2.3–3.0)	–	Yang et al., 2025; This study

[a] Range: min-max (mean); [b] Log K_d value: mean ± standard deviation.

Table S13. Comparison of PFASs in sediments obtained from this study and previous studies (ng g^{-1} dw).

Regions	Sampling Year	*n* [a]	PFHxA	PFHpA	PFOA	PFNA	PFDA	PFUnDA	PFDoDA	PFTriDA	PFTeDA	br-PFOSK	other PFASs	∑PFASs	References
Bohai Sea, China	2017	30	0.09	0.13	0.46	0.16	0.06	0.10	0.03	NA[b]	NA	<LOD[c]	0.74	1.8	Zhao et al., 2020
Yangtze River Estuary	2022	20	0.0045	<LOD	0.33	0.06	0.05	0.09	0.01	0.02	<LOD	<LOD	0.68	1.3	Li et al., 2024
Yellow Sea (YS)	2011-2012	66	NA	<LOD	0.19	0.08	0.02	0.08	0.01	NA	NA	0.09	0.02	0.49	Gao et al., 2014
East China Sea (ECS)	2011-2012	71	NA	<LOD	0.18	0.06	0.03	0.06	0.06	NA	NA	0.10	0.03	0.52	Gao et al., 2014
East China Sea	2023	27	0.02	0.007	0.31	0.07	0.05	0.06	0.02	NA	NA	0.13	0.20	0.85	Zhu et al., 2025
Korea coast	2018	50	0.01	0.002	0.06	0.02	0.02	0.05	0.01	0.03	0.005	0.05	0.06	0.33	Lee et al., 2020
Bukhan River	2012	3	0.02	<LOD	0.04	0.02	0.01	0.04	0.07	NA	NA	0.04	0.01	0.25	Lam et al., 2014
Nakdong River	2012	3	0.01	<LOD	0.06	0.01	0.05	0.06	0.08	NA	NA	0.16	0.0	0.43	Lam et al., 2014
Yeongsan River	2012	3	<LOD	<LOD	0.02	0.12	0.03	0.03	0.07	NA	NA	0.07	0.01	0.35	Lam et al., 2014

[a] n: Sample numbers; [b] NA: Not available; [c] <LOD: Below limit of detection.

Supplementary Figures

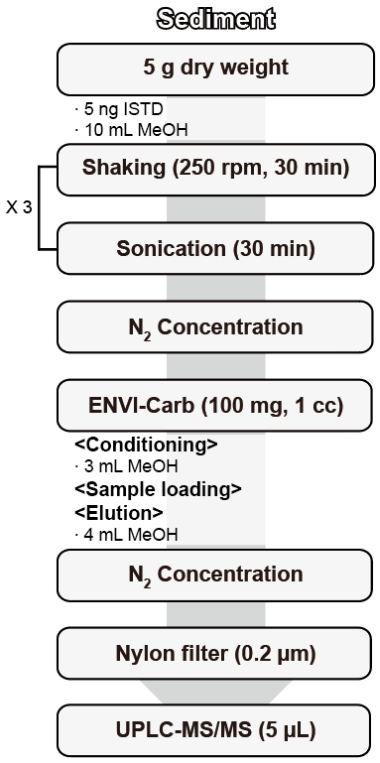

Fig. S1. Analytical procedures for per- and polyfluoroalkyl substances (PFASs) in sediment samples.

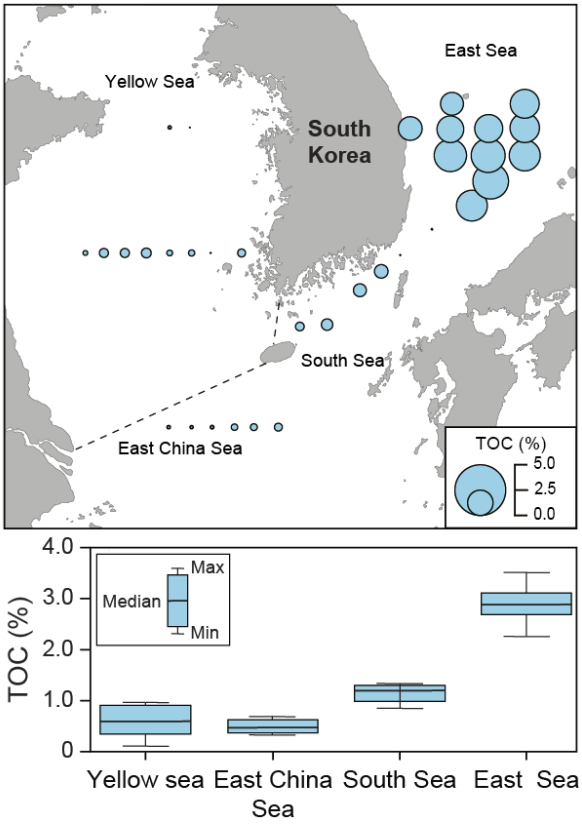

Fig. S2. Distributions of total organic carbon (TOC) contents in sediments from the Yellow Sea, East China Sea, South Sea, and East Sea.

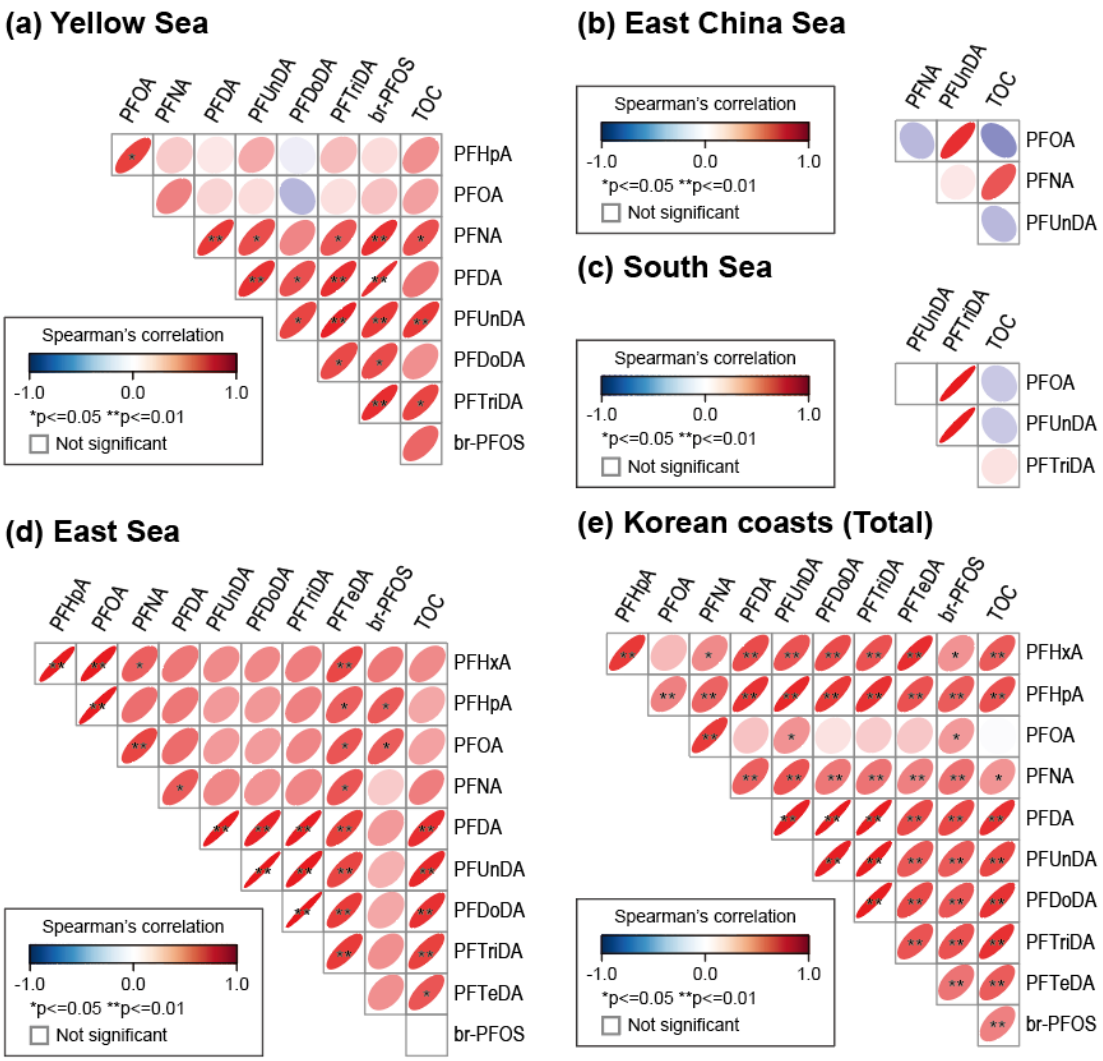

Fig. S3. Correlation between PFASs and OC in sediments from **(a)** Yellow Sea, **(b)** East China Sea, **(c)** South Sea, **(d)** East Sea, and **(e)** regional seas of Korea (total).

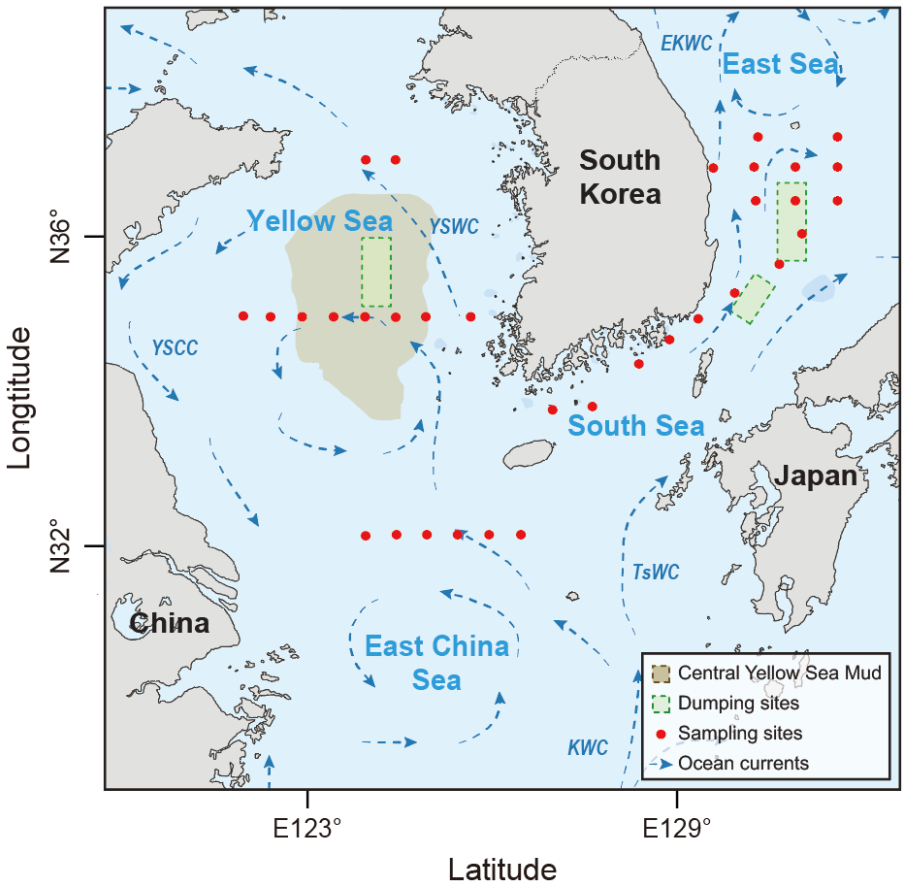

Fig. S4. Sampling sites and nearby current distribution in this study [YSCC: Yellow Sea Coastal Current; YSWC: Yellow Sea Warm Current; KWC: Kuroshio Warm Current; TsWC: Tsushima Warm Current; and EKWC: East Korean Warm Current (Guo et al., 2006; Hu et al., 2011; Lee et al., 2009)].

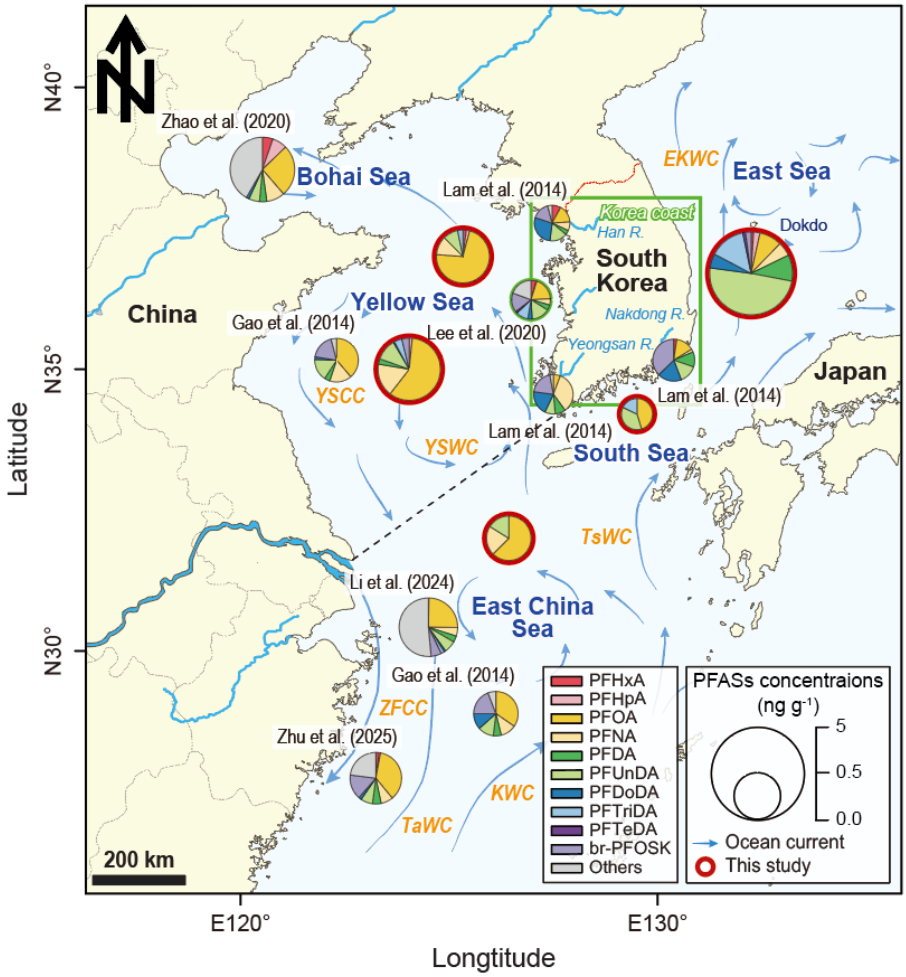

Fig. S5. Comparison of the concentrations and composition of PFASs in sediments collected from freshwater, coastal areas, and regional seas of South Korea.

References

Campo, J., Pérez, F., Masiá, A., Picó, Y., Farré, M.l., Barceló, D., 2015. Perfluoroalkyl substance contamination of the Llobregat River ecosystem (Mediterranean area, NE Spain). Sci. Total Environ. 503–504, 48–57. https://doi.org/10.1016/j.scitotenv.2014.05.094.

Diao, J., Chen, Z., Su, C., Wang, J., Zheng, Z., Sun, Q., Wang, L., Bi, R., Wang, T., 2023. Legacy and novel perfluoroalkyl substances in major economic species of invertebrates in South China Sea: Health implication from consumption. Mar. Pollut. Bull. 192, 115112. https://doi.org/10.1016/j.marpolbul.2023.115112.

Gao, Y., Fu, J., Zeng, L., Li, A., Li, H., Zhu, N., Liu, R., Liu, A., Wang, Y., Jiang, G., 2014. Occurrence and fate of perfluoroalkyl substances in marine sediments from the Chinese Bohai Sea, Yellow Sea, and East China Sea. Environ. Pollut. 194, 60–68. https://doi.org/10.1016/j.envpol.2014.07.018.

Guo, C., Zhang, Y., Zhao, X., Du, P., Liu, S., Lv, J., Xu, F., Meng, W., Xu, J., 2015. Distribution, source characterization and inventory of perfluoroalkyl substances in Taihu Lake, China. Chemosphere 127, 201–207. https://doi.org/10.1016/j.chemosphere.2015.01.053.

Guo, Z., Lin, T., Zhang, G., Yang, Z., Fang, M., 2006. High-resolution depositional records of polycyclic aromatic hydrocarbons in the central continental shelf mud of the East China Sea. Environ. Sci. Technol. 40, 5304–5311. https://doi.org/10.1021/es060878b.

Hu, L., Lin, T., Shi, X., Yang, Z., Wang, H., Zhang, G., Guo, Z., 2011. The role of shelf mud depositional process and large river inputs on the fate of organochlorine pesticides in sediments of the Yellow and East China seas. Geophys. Res. Lett. 38. https://doi.org/10.1029/2010GL045723.

Lam, N.-H., Cho, C.-R., Lee, J.-S., Soh, H.-Y., Lee, B.-C., Lee, J.-A., Tatarozako, N., Sasaki, K., Saito, N., Iwabuchi, K., Kannan, K., Cho, H.-S., 2014. Perfluorinated alkyl substances in water, sediment, plankton and fish from Korean rivers and lakes: A nationwide survey. Sci. Total Environ. 491–492, 154–162. https://doi.org/10.1016/j.scitotenv.2014.01.045.

Lee, J.-W., Lee, H.-K., Lim, J.-E., Moon, H.-B., 2020. Legacy and emerging per- and polyfluoroalkyl substances (PFASs) in the coastal environment of Korea: Occurrence, spatial distribution, and bioaccumulation potential. Chemosphere 251, 126633. https://doi.org/10.1016/j.chemosphere.2020.126633.

Lee, J.-Y., Kang, D.-J., Kim, I.-N., Rho, T., Lee, T., Kang, C.-K., Kim, K.-R., 2009. Spatial and temporal variability in the pelagic ecosystem of the East Sea (Sea of Japan): A review. J. Mar. Syst. 78, 288–300. https://doi.org/10.1016/j.jmarsys.2009.02.013.

Li, L., Han, T., Li, B., Bai, P., Tang, X., Zhao, Y., 2024. Distribution Control and Environmental Fate of PFAS in the Offshore Region Adjacent to the Yangtze River Estuary─ A Study Combining Multiple Phases Analysis. Environ. Sci. Technol. 58, 15779–15789. https://doi.org/10.1021/acs.est.4c03985.

Liu, J.-J., Zhang, Y.-H., Li, F., Sun, J., Yuan, S.-J., Zhang, P.-D., 2024. Contamination status, partitioning behavior, ecological risks assessment of legacy and emerging per- and polyfluoroalkyl substances in a typical heavily polluted semi-enclosed bay, China. Environ. Res. 247, 118214. https://doi.org/10.1016/j.envres.2024.118214.

Tang, A., Zhang, X., Li, R., Tu, W., Guo, H., Zhang, Y., Li, Z., Liu, Y., Mai, B., 2022. Spatiotemporal distribution, partitioning behavior and flux of per- and polyfluoroalkyl substances in surface water and sediment from Poyang Lake, China. Chemosphere 295, 133855. https://doi.org/10.1016/j.chemosphere.2022.133855.

Wang, G., Xing, Z., Liu, S., Chen, H., Dong, X., Guo, P., Wang, H., Liu, Y., 2024. Emerging and legacy per- and polyfluoroalkyl substances in Daling River and its estuary, Northern China. Mar. Pollut. Bull. 199, 115953. https://doi.org/10.1016/j.marpolbul.2023.115953.

Wang, Q., Tsui, M.M.P., Ruan, Y., Lin, H., Zhao, Z., Ku, J.P.H., Sun, H., Lam, P.K.S., 2019. Occurrence and distribution of per- and polyfluoroalkyl substances (PFASs) in the seawater and sediment of the South China sea coastal region. Chemosphere 231, 468–477. https://doi.org/10.1016/j.chemosphere.2019.05.162.

Xiao, S.-K., Wu, Q., Pan, C.-G., Yin, C., Wang, Y.-H., Yu, K.-F., 2021. Distribution, partitioning behavior and potential source of legacy and alternative per- and polyfluoroalkyl substances (PFASs) in water and sediments from a subtropical Gulf, South China Sea. Environ. Res. 201, 111485. https://doi.org/10.1016/j.envres.2021.111485.

Yang, S., Gwak, J., Kim, M., Cha, J., Kim, Y., Lee, Y., Moon, H.-B., Hong, S., 2025. Spatial and vertical distribution of per- and polyfluoroalkyl substances (PFASs) in the water columns of the regional seas of South Korea. Chemosphere 370, 144042. https://doi.org/10.1016/j.chemosphere.2024.144042.

Zhang, Y., Meng, W., Guo, C., Xu, J., Yu, T., Fan, W., Li, L., 2012. Determination and partitioning behavior of perfluoroalkyl carboxylic acids and perfluorooctanesulfonate in water and sediment from Dianchi Lake, China. Chemosphere 88, 1292–1299. https://doi.org/10.1016/j.chemosphere.2012.03.103.

Zhao, Z., Cheng, X., Hua, X., Jiang, B., Tian, C., Tang, J., Li, Q., Sun, H., Lin, T., Liao, Y., Zhang, G., 2020. Emerging and legacy per- and polyfluoroalkyl substances in water, sediment, and air of the Bohai Sea and its surrounding rivers. Environ. Pollut. 263, 114391. https://doi.org/10.1016/j.envpol.2020.114391.

Zhu, J., Fu, Y., Hu, H., Zhong, Y., Ma, X., Zhu, Y., Zhou, F., Pan, Y., Ma, Y., 2025. Regulation of terrestrial input and ocean processes on the occurrence and transport of traditional and emerging per- and polyfluoroalkyl substances in the inner shelf of the East China Sea. Water Res. 268, 122606. https://doi.org/10.1016/j.watres.2024.122606.

Zhu, Z., Wang, T., Wang, P., Lu, Y., Giesy, J.P., 2014. Perfluoroalkyl and polyfluoroalkyl substances in sediments from South Bohai coastal watersheds, China. Mar. Pollut. Bull. 85, 619–627. https://doi.org/10.1016/j.marpolbul.2013.12.042.